# THE INFLUENCE OF CHROMOSOME CONTENT ON THE SIZE AND SHAPE OF SPERM HEADS IN *DROSOPHILA MELANOGASTER* AND THE DEMONSTRATION OF CHROMOSOME LOSS DURING SPERMIOGENESIS[1]

ROBERT WALTER HARDY[2]

*Department of Biology, University of California at San Diego, La Jolla, California 92037*

## ABSTRACT

The volumes of sperm heads were estimated from three-dimensional reconstructions of serially sectioned bundles of nearly mature spermatid nuclei. Cysts from males in which all sperm are expected to have comparable amounts of chromatin *(X/Y* and *In(3LR)/+)* show unimodal frequency distributions of nuclear volumes, whereas cysts from males in which meiotic segregation is expected to deliver unequal amounts of chromatin material to spermatid nuclei show two *(XY/O* and *XY/Y)* or more *(T(2;3)/+* and *C(2L);C(2R))* modes. The mean volumes of the subpopulations in these cases are related in the same proportions as the metaphase lengths of their chromosomal complements. Thus the volumes of sperm nuclei are proportional to their DNA content. Sperm head shape, on the other hand, does not appear to be very sensitive to chromosomal constitution, as heads of different size do not vary greatly in shape.————The numbers of sperm heads in the various size classes in a cyst depart from mendelian expectations; these departures are caused by the elimination, during individualization, of chromosomes contained within micronuclei that are formed in spermatids at the end of the second meiotic division. The effect of this chromosome loss is to increase the proportion of nullosomic gametes in the sperm pool.————The relative frequencies of *XY*-bearing and nullo-*X*, nullo-*Y* sperm in *XY/O* males were estimated from the volume measurements. Taking this estimate as a measure of the fertilizing population, it is possible to infer from the change in sex ratio over time following insemination, that *XY*-bearing sperm have an advantage of 1.5 over nullo-*X*, nullo-*Y* sperm in leaving the seminal receptacle of the female for fertilization of ova.

P REVIOUS attempts to relate sperm size to chromosome constitution in Drosophila have used the light microscope. These studies were limited to measurements of either length total (BEATTY and SIDHU 1970) or of parts such as head or flagellum (HERSKOWITZ and MULLER 1954; SIDHU 1964; BEATTY and SIDHU 1967; BEATTY and BURGOYNE 1971). This report examines the dimensions of spermatozoan nuclei of *Drosophila melanogaster* by electron microscopic examination of serial sections of bundles of nearly mature sperm heads.

The study has three objectives: the first is to determine what effect changing the quantity of chromatin that a spermatid nucleus contains has on its volume and morphology. Whereas most recent investigations of nuclear length of Drosophila sperm are concerned with detecting effects of genetic background (BEATTY and SIDHU 1967; BEATTY and BURGOYNE 1971), HERSKOWITZ and MULLER (1954) examined the effect of the quantity of chromatin on sperm head length. They measured the head lengths of spermatozoa produced by wild-type males and males having an attached $XY$ chromosome and no free $Y$ chromosome. On the hypothesis that chromosomes are tandemly arranged within the sperm nucleus, they expected sperm of two lengths from the second kind of male. Although they failed to find a bimodal distribution in either case, the variance of the second distribution was greater than the first. They concluded that chromosomes are not tandemly arranged and accounted for their observations by assuming a model for head shape, in which head length is proportional to the cube root of the volume of chromatin contained within.

The second objective is to determine the effect on sperm head morphology of altering the arrangement of the chromatin in relation to the centromere of a chromosome or between the centromeres of different chromosomes. It is known in at least one animal, a plethodontid salamander, that the centromeric regions of the chromosomes have a specific location at the base of the sperm nucleus (MACGREGOR and WALKER 1973).

The third objective is to determine the basis of the unequal recovery of reciprocal meiotic products exhibited by $XY/O$ males. SANDLER and BRAVER (1954) suggested that the reduced recovery of the $XY$ chromosome in the progeny of such males is due to meiotic loss of the attached $XY$ chromosome. Later LINDSLEY and SANDLER (1958), studying the segregation of an $XY$ chromosome from small free-$X$ duplications, detected no chromosome loss and suggested sperm dysfunction as the only explanation for the unequal recovery observed in their experiments. Hence, two explanations for the reduced recovery of the $XY$ chromosome have been proposed, chromosome loss or sperm dysfunction. In $XY/O$ males either hypothesis can account for the observations, but when the $XY$ chromosome has a pairing partner it is necessary to postulate sperm dysfunction.

The results reported in this paper indicate that the volume of a sperm nucleus is proportional to its DNA content and its shape is unaffected by DNA content and chromosome constitution. In addition, the results demonstrate that chromosome loss is responsible for the deficiency of $XY$-bearing offspring observed in progenies of $XY/O$ males.

## MATERIALS

Spermiogenesis in *Drosophila melanogaster* has recently been the subject of intense morphological study in the laboratories of several investigators. A brief review of their findings seems essential to bring this study into perspective.

The testes are tubular, closed at the apical end where the germinal stem cells are located, and measure about 2 mm long and .1 mm wide (Figure 1a). As the germ cells mature through the various stages of gonial proliferation and spermatogenesis, their nuclei are displaced toward
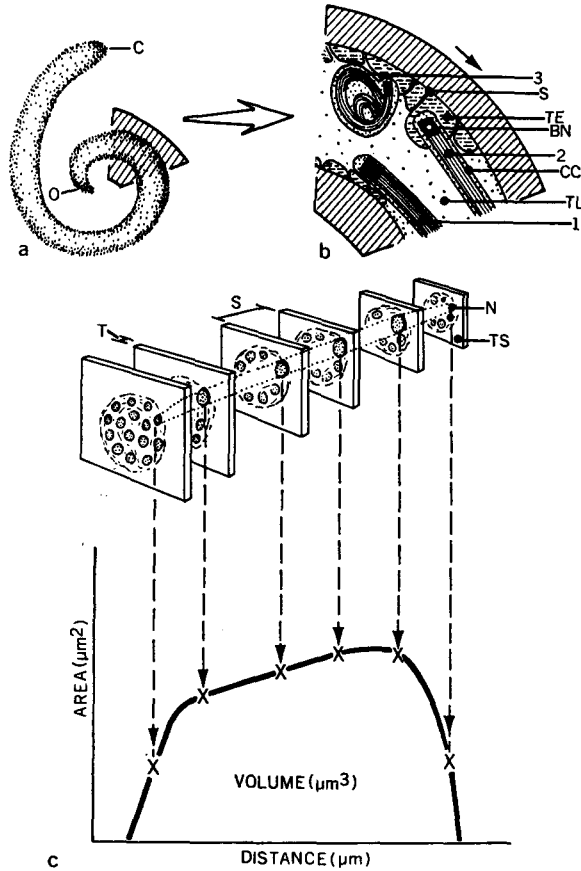
FIGURE 1.—The method of determining the volume and shape of a sperm head. (a) A schematic of the testis indicating the region in which the spermatid nuclei, in the stage of development used in this study, are located. C, closed apical end; O, open basal end, which connects with the testicular duct. (b) An enlargement of the region cross-hatched in 1a. The nuclei of spermatid bundles (1,2,3) are represented by dark thick rectangles, BN, and their tails by thin lines extending away from the nuclei. The cyst cells surrounding each bundle, CC, and the terminal epithelial cells, TE, are shown. Bundle 1—before entrapment; Bundle 2—after entrapment but before coiling; Bundle 3—coiling; S, testis sheath; TL, testicular lumen. The epon block was oriented for sectioning so that sectioning advanced in the direction of the arrow; toward the closed apical end. (c) A schematic showing the method of plotting the distribution of cross-sectional area along the length of the nucleus. The area estimates, X, are derived using a computer as described in the text. TS, thin section; T, section thickness; S, distance between sections. Only 15 nuclei are drawn, one of which is followed through all the thin sections. The area under the curve estimates the nuclear volume, and the shape of the curve reflects the nuclear shape.

the open end of the testis. After completion of spermiogenesis the motile sperm pass through the testicular duct at the basal end of the testis into the seminal vesicle where they remain until ejaculation. Early accounts of the cytology and ultrastructure of the testis are given by COOPER (1950) and BAIRATI (1967), respectively.

Groups of germinal nuclei mature synchronously within an envelope composed of two or more cyst cells (COOPER 1950; TOKUYASU, PEACOCK and HARDY 1972a,b). The 64 members of a

group are derived by 4 mitotic and 2 meiotic divisions from a single gonial cell. When the 16 primary spermatocytes enter meiosis, the cyst is at about the mid-point along the length of the testis. After meiosis, elongation of the 64 spermatids results in the displacement of the nuclei toward the base of the testis as the tails extend toward the apical end. Tokuyasu, Peacock and Hardy (1972a) reported that the nuclei of fully elongated spermatids are located in the region of the testis approximately 0.2–0.4 mm from the basal opening. This region, which is cross-hatched in Figure 1a, contains nuclei belonging to bundles of spermatids in later stages of spermatogenesis.

After meiosis, the various parts of the spermatids go through several identifiable changes in morphology. For descriptive purposes we recognize four stages that take place sequentially during spermatid development: elongation, maturation, individualization, and coiling. After individualization, the nuclei are highly condensed and do not differ significantly from nuclei of sperm in the seminal vesicle. Accounts of the changes in the ultrastructure of cellular organelles during these processes were also given by Tates (1971) and by Stanley et al. (1972).

After individualization and early in the coiling stage the cyst cell surrounding the nuclear portion of the spermatid bundle becomes closely associated with the terminal epithelium—a single layer of columnar cells lining the basal 10% of the testis (Figure 1b; Tokuyasu, Peacock and Hardy 1972b). The association is thought to provide a means of anchoring the nuclear regions of the spermatids while their tail regions are being retracted from the lumen into the base of the testis.

The release of the spermatids from the bundle follows the completion of coiling. After release the sperm from different bundles become mixed. The coiling stage is the last time that the meiotic products can be found together in such a way that their morphologies can be compared and correlated with the expected segregation of chromosomes during the meiotic division; i.e., by using material in this stage the investigator is not forced to examine a random sample but rather can examine all the products of the 16 meiotic divisions. The advantage of the method outlined in this paper is analogous to that of scoring tetrads compared with scoring random spores for analyzing the meiotic segregation of chromosomes.

In the late coiling stage, as identified by the presence of minute tubules in the space between the spermatids (Tokuyasu, Peacock and Hardy 1972b), sperm nuclei are often curved and unsuitable for obtaining good cross-sections at all levels. However, sperm nuclei in the early coiling stage are considered ideal.

## METHOD OF NUCLEAR RECONSTRUCTION

Thin sectioning was done on entire bundles, but not all sections were viewed; rather, representative sections were selected for viewing in the electron microscope (Figure 1c). The thickness of each section, as well as the interval between selected sections ($T$ and $S$ in Figure 1c), were estimated from the interference color of the sections while they were floating on the surface of the sectioning trough (Peachey 1958). The cross-sectional area of each nucleus in a section was estimated with the aid of a computer, and then utilizing data from all sections sampled the cross-sectional areas of each spermatid were plotted as a function of their positions along the length for each nucleus as shown in Figure 1c. The area under the resulting curve provides an estimate of nuclear volume. The shape of the curve indicates how the mass of the sperm head is distributed along its length and thus provides an estimate of one component of head shape. Since sperm nuclei are roughly circular in cross-section (Figure 2), except for short lengths at the ends where acrosomes and axonemes are inserted (Perotti 1969), these curves provide relatively accurate indices of nuclear shape.

*Electron microscopy and estimation of length*: Testes of 3-day-old unmated males were dissected in cold 2% gluteraldehyde in 0.1 M $PO_4$ buffer at pH 7.4. After 2 hours in gluteraldehyde at 4° they were washed with buffer three times and transferred into cold 2% $OsO_4$ in 0.1 M $PO_4$ buffer for two hours. Ethanol dehydration and a propylene oxide series preceded embedding in Epon 812. Sections were cut on a Sorvall-Porter Blum MT2-B ultramicrotome using a diamond knife and were decompressed with a Polaron heat pen. The thickness of each section floating in the knife boat was estimated after decompression by comparing its interference
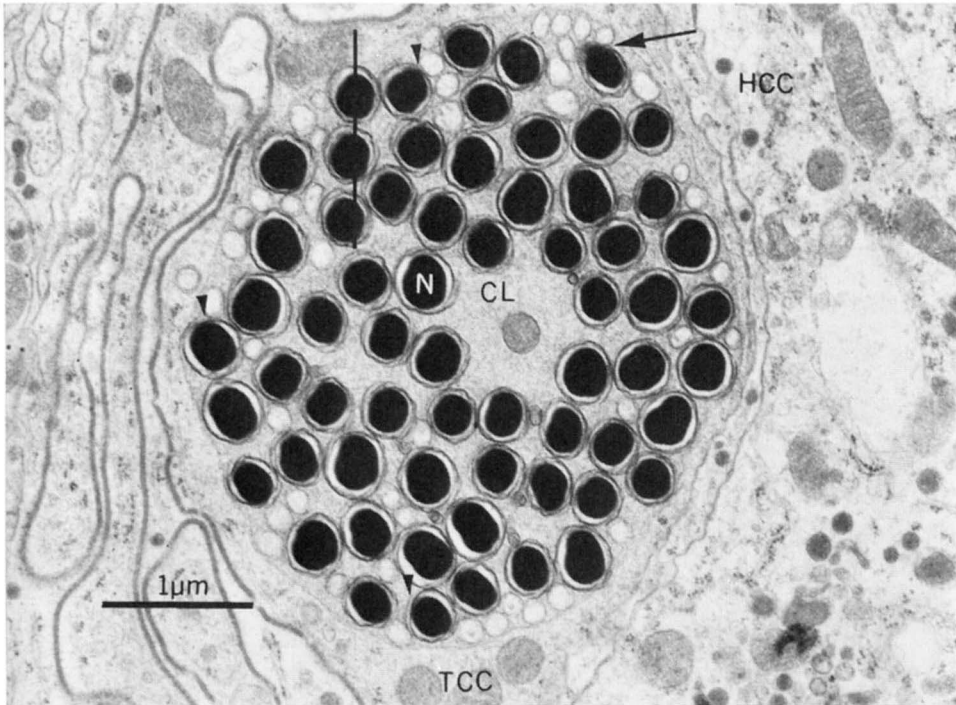
FIGURE 2.—An electron micrograph of a cross-section through a bundle of 63 spermatid nuclei in the early coiling stage. The arrow points to a nucleus in which the acrosome insertion is seen. Three places are indicated by arrowheads where the plasma membrane closely approaches the nucleus. The vertical line represents the type of scan shown in Figure 3. N, nucleus; HCC, head cyst cell; TCC, tail cyst cell; CL, cyst lumen.

color to the color chart supplied with the microtome. With this method the thickness can be estimated to within 10–20% (PEACHEY 1958)—this doubtlessly accounts for the variation in estimates of lengths of nuclei with the same genetic content (Table 1). The preferred thickness was 0.1 $\mu$m. Sections to be photographed were mounted singly on a 0.8 mm monohole grid having a support film. All sections were stained with 2% uranyl acetate and REYNOLDS' lead citrate (1963) before viewing in the Phillips EM 300. Photographs were made on film sheets rather than glass plates to allow mounting of the negatives on the drum of the scanning densitometer. The magnification was set at 10,000.

The Epon blocks were trimmed to allow cross-sections of the testis to be obtained at about 0.3 mm from the testicular opening. Sectioning was toward the closed end of the testis (C in Figure 1a; arrow in Figure 1b) beginning at about 0.2 mm from the open end with 0.25 $\mu$m thick sections. The thick sections were stained with methylene blue and observed in the light microscope. The first sections contain many sperm tails of coiling bundles, but as sectioning continues these become fewer. Thin sections were interspersed among the thick ones and monitored in the electron microscope for the presence of acrosomes. Once acrosomes were encountered thin sections were cut continually and viewed intermittently to monitor bundle orientation. Sectioning was continued until cross-sections of sperm tails were found in place of all nuclei.

*Estimation of cross-sectional area*: The computerized system for measurement of nuclear areas is based on detecting the difference in density between the nuclear images and background structures. The plasma membrane is often closely opposed to the nucleus (arrowheads in Figure 2) and interferes with the measurement of nuclear cross-sectional area. This difficulty was overcome by opaquing the membrane image with India ink.

TABLE 1

*Summary of the results of seven experiments to determine nuclear volumes and lengths by reconstruction from electron micrographs of serial cross-sections*

| Genotype | Number in group | Nuclear length | | | Nuclear volume | | | |
|---|---|---|---|---|---|---|---|---|
| | | Mean ($\mu$m) | Standard deviation ($\mu$m) | Coefficient of variation (%) | Mean ($\mu$m)$^3$ | Standard deviation ($\mu$m)$^3$ | Coefficient of variation (%) | Ratio of means |
| Canton-S | 61 | 11.05 | .57 | 5.1 | .685 | .027 | 4.1 | — |
| $Y^sX \bullet Y^L/O$ | | | | | | | | |
| Bundle A | 37 | 7.55 | .37 | 4.9 | .456 | .011 | 2.4 | |
| | 26 | 8.48 | .30 | 3.6 | .647 | .015 | 2.4 | 1.42 |
| Bundle B | 1 | 4.42 | — | — | .184 | — | — | |
| | 41 | 6.97 | .55 | 7.9 | .406 | .020 | 5.1 | 2.20 |
| | 20 | 8.26 | .58 | 7.0 | .585 | .017 | 2.9 | 1.44 |
| $Y^sX \bullet Y^L/y^+Y$ | 1 | 8.48 | — | — | .444 | — | — | |
| | 30 | 9.50 | .353 | 3.7 | .571 | .020 | 3.4 | 1.29 |
| | 30 | 9.83 | .484 | 4.9 | .642 | .015 | 2.4 | 1.12 |
| | 1 | 11.08 | — | — | .776 | — | — | 1.21 |
| $C(2L);C(2R)$ | 15 | 6.08 | .624 | 10.3 | .289 | .025 | 8.6 | |
| | 35 | 7.47 | .402 | 5.4 | .420 | .022 | 5.3 | 1.30 |
| | 8 | 8.18 | .212 | 2.6 | .547 | .016 | 2.9 | 1.45 |
| $In(3LR)/+$ | 62 | 9.64 | .372 | 3.9 | .475 | .017 | 3.5 | |
| $T(2;3)lt^{mr}/+$ | 12 | 9.13 | .469 | 5.1 | .444 | .007 | 1.6 | — |
| | 40 | 9.54 | .544 | 5.7 | .516 | .025 | 4.8 | 1.16 |
| | 12 | 10.23 | .567 | 5.5 | .597 | .017 | 2.9 | 1.16 |

The digital scanning-densitometer described by Xuong (1969) connected to an IBM 1800 computer equipped with disk memory was used to measure the area of the nuclear images. The handling of the data is divided into 4 steps: (1) conversion of electron images on the negative to digital values; (2) establishment of a density threshold for distinguishing nuclear images from background; (3) search for the contours of the nuclear images and computation of their enclosed areas; (4) plotting the nuclear contours for identifying each nucleus in successive negatives.

1. The negatives of one bundle of nuclei to be scanned are mounted singly on the scanning-densitometer and the scanning program is initiated. The electron images are converted to a digitized raster having $600 \times 600$ elements or cells graded from 0 to 255. The digital value in each cell represents the integrated optical density of a 100 $\mu m^2$ area of the negative (Xuong 1969). The digitized raster is stored on disk for further processing.

2. Recognition of nuclear area by the search program (step 3) is facilitated by an operator-computer interactive program that eliminates background images. The nuclear areas in the negatives are less dense than background. Consequently, cells of the raster that are within these areas will have small digital values. The operator enters a number, the *threshold*, that is compared to the digital value of each cell. Digital values greater than threshold are converted to "0" for background; digital values equal to or less than threshold are converted to "1" for data. The results of the comparisons are displayed on an oscilloscope to allow the operator to compare a nuclear area in the negative to the cells that the computer has recognized as data. If a discrepancy exists the threshold value is adjusted until one is found that allows the computer to recognize only data cells belonging to a nucleus.
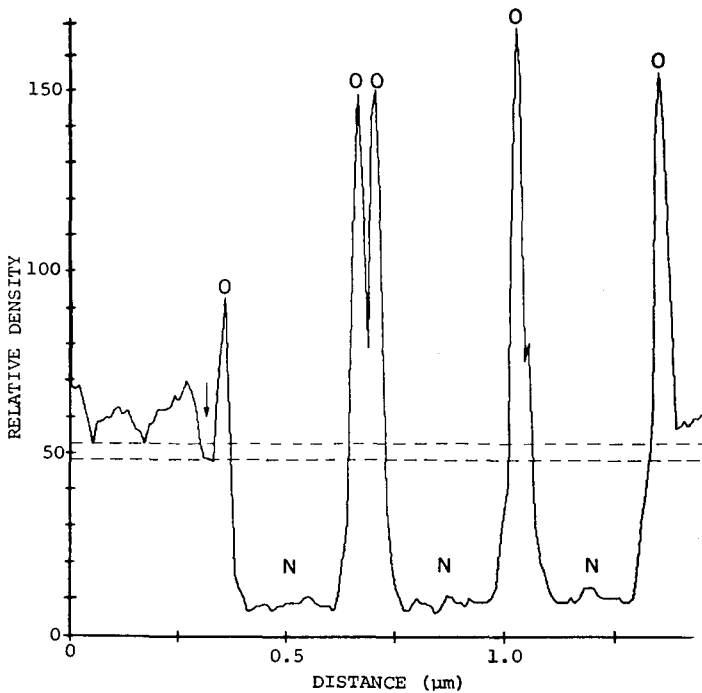


FIGURE 3.—A graph of the relative densities measured in a negative along a portion of a digital scan as it traverses a spermatid bundle. A similar line is shown in Figure 2. The dashed lines indicate the range over which a threshold is selected (see text). Densities less than the threshold value are included within the areas outlined as shown in Figure 4. The small arrow indicates a background body that could appear as one of the five shown in Figure 4. O, opaqued plasma membrane; N, spermatid nuclei.

Figure 3 is a graph of the relative densities represented by the digital values of about 150 sequential cells from one scan (e.g., the vertical line in Figure 2). In practice, a threshold value is chosen in a range over which estimated cross-sectional area is almost insensitive to changes in threshold (between the dashed lines in Figure 3). To save computer time only alternate X and Y lines of the 600 × 600 raster were used. The consequences of using only ¼ of the cells is to make the contour and area estimates more coarse, resulting in a higher variance. The coarseness affects area estimates at the periphery of a nuclear profile; hence, smaller areas will be less accurately estimated than larger ones. The variance was empirically determined by repeated measurements of large and small areas at a fixed threshold value. The smallest areas this system measured, approximately a 1-mm diameter circle on the negative, had a coefficient of variation of about 3% and areas approximately ten times larger, about 2.5%. These findings suggest an appreciable portion of the coefficient of variation found in the experiments may be due to the computer estimating method. Use of more than 90,000 of the 360,000 digitized cells would decrease this variation.

3. In order to estimate the cross-sectional areas of the nuclei the cells of the 300× 300 raster are examined sequentially by the search program until a cell is found that has a 1, a data cell; then the program uses that cell as the focus for a systematic search of the eight adjoining cells. If no data cells are found the sequential examination is resumed; if, on the other hand, one of the adjoining cells is a data cell, it will become the focus of a search of its eight adjoining cells. The focus-search-shift cycle continues until the starting data cell is reached. The result is that the perimeter of a nuclear contour is delineated. The nuclear area is defined as the total number of cells within the perimeter. The computer operates in a way analogous to a planimeter. After the contour is assigned a reference number and the coordinates of its perimeter are stored for processing in step 4, the scan is resumed. A card is punched for each nuclear contour which contains its reference number, area, the coordinates of its center, and an operator-assigned number indicating its position along the length of the sperm head.

The minimum area measured was chosen so that its image on the negative was at least 100 times that of the densitometer aperture. This minimum corresponds to circular areas of about 0.01 $\mu$m$^2$ which are near both nuclear ends (e.g., Figure 7).

4. A plotting program transforms the computer-stored coordinates into plots of the contours of all the nuclear areas from one negative, identifying each with its reference number. A sample of such output is presented in Figure 4. The plots are used to identify the successive cross-sections of each nucleus in a bundle.

The measurement of area is subject to several sources of error which may be subdivided into those attributable to electron microscopy and those attributable to the computer system. The latter can be estimated empirically and were discussed in section 2 above. The sources of inaccuracy in the microscopy may include such diverse sources as tissue preparation procedures, section compression during cutting, staining properties, microscope magnification, and so forth. These types of errors can be minimized or at least systemized by adoption of standard procedures. A more significant but perhaps less obvious source of error results from obliqueness in the plane of sectioning *versus* the long axis of the sperm nucleus. This can best be seen by considering the sperm nucleus as a circular cylinder (which it closely approximates over most of its length). If the plane of sectioning is normal to the axis of the cylinder, then the cross-section is circular; if the plane of sectioning is oblique, then the cross-section is elliptical. If the microscopic section were infinitely thin, then both the sum of circular cross-sections in a right-sectioned circular cylinder and the sum of elliptical cross-sections in an obliquely sectioned circular cylinder would estimate the volume of the cylinder. However, the sections are not infinitely thin. In fact their thickness (0.1 $\mu$m) is comparable to the width of the sperm nuclei 0.1– 0.4 $\mu$m). Assuming uniform staining throughout a section, the photographic image whose area is being estimated is the planer projection of a three-dimensional segment of the sperm nucleus. Although the projection of a right section of a cylinder is congruent with the circular cross-section, the projection of an oblique section is larger than the ellipse of cross-section by an amount *td tan*Θ where *d* is the diameter of the cylinder, *t* is the thickness of the section and Θ is the angle of departure of the longitudinal axis of the cylinder from normality to the plane of section (Figure 5). Using the same notation, the area of the elliptical cross-section is *0.25 $\pi d^2$ sec*Θ;
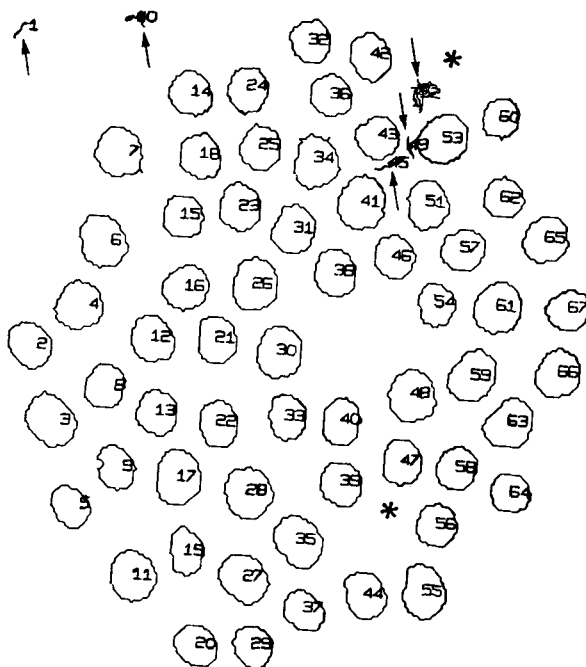
FIGURE 4.—Computer output from processing a negative of a cross-section acrosomal to that shown in Figure 2. Sixty-one arbitrarily numbered nuclear outlines are shown. The asterisks indicate the location of the acrosomes of the two nuclei present in Figure 2 but absent in this figure. The five small arrows indicate background bodies.

thus the total area of the image projected is $0.25\ \pi d^2\ sec\Theta\ +\ td\ tan\Theta$. Tilting a normally sectioned bundle of sperm (i.e., Figure 17) through 10° is estimated to cause less than a 10% overestimate of nuclear volume. In order to minimize this source of error it is desirable to keep $\Theta$ as close to zero as possible and sections as thin as practical. In oblique sections the rate at which optical density falls off along the axis of tilt at the ends of the planar image gives a crude estimate of the angle $\Theta$. Unless noted otherwise, in the following experiments $\Theta$ is estimated to be between 0° and 10°. No corrections were made to the data because of the tilt angle.

It should be pointed out that an uncontrollable source of variation and error is caused by departures from parallelism of the nuclei within a bundle. The result of such departures is that $\Theta$ will not be the same for all nuclear areas seen in a cross-section of a bundle. The maximum contribution to $\Theta$ from this source is estimated to be about 4°.

*Estimation of volume*: The plot of the cross-sectional area as a function of distance and the calculation of volume for each nucleus is accomplished by the following steps: (1) All the punch cards belonging to a specific nucleus are manually assembled and two cards are added to flag the nuclear limits by defininirg the location along the bundle of the first section at either end of a spermatid head region which contains no nucleus. Their effect is to adjust for areas of less than 0.01 $\mu m^2$ that were cut out by the search program. (2) Reconstruction of each nucleus is accomplished by a program that plots the area of each nuclear cross-section at its correct position along the length of the bundle and connects the points. The area under the curve (Figure 1c) represents the nuclear volume and, as previously mentioned, the shape of the curve indicates the distribution of nuclear mass along the length of the nucleus.

When the volumes for all the nuclei were determined, a frequency distribution was inspected for obvious groupings. The results of the genetic crosses may in some cases help to clarify how many members belong to a group. The distributions of nuclear volumes in all bundles examined
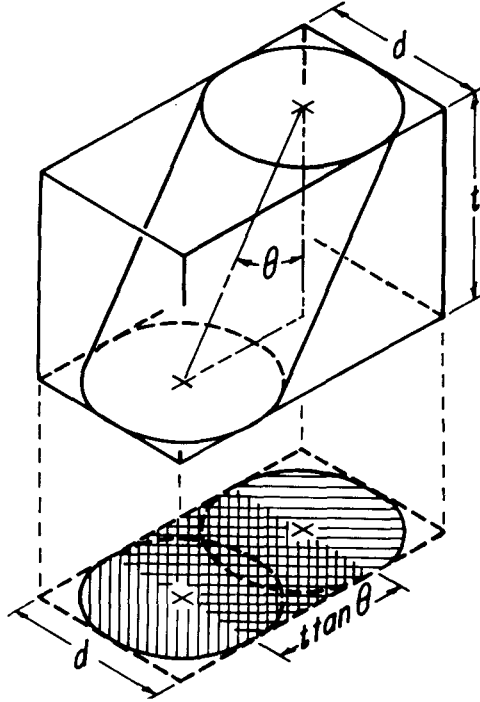
FIGURE 5.—The projection of an oblique section of a right circular cylinder onto a flat surface. The overestimation (double-hatched area) of the true elliptical cross-sectional area (single hatched area) is $td\ tan\Theta$ where $d$ is the diameter of a sperm nucleus; $t$ is the thickness of the section; and $\Theta$ is the angle of tilt.

were tested for normality by testing for significant departures from expected values of the co-efficients of skewness and kurtosis. The mean, standard deviation, and coefficient of variation were computed and when the distribution of volumes obviously consisted of two or more populations with different modes (e.g., Figure 8), these statistics were computed for the nuclei in each mode, even though in some cases the modes had insufficient numbers to test for normality.

In order to determine the curve that best represents all the nuclei within each group, a program brings the curves for all the nuclei into register by using the most anterior limit of the axoneme insertion as a reference point which in turn is assigned an arbitrary position on the abscissa. Then, the mean cross-sectional area and its 95% confidence limits are computed at 0.1 $\mu$m intervals along the length axis. These values are plotted for each group of nuclei (e.g., Figure 9). Inaccuracies in choosing the reference points tend to make the area under the average curve slightly larger than that of the individual curves; therefore, mean volumes were calculated from the individual curves.

Sperm with the same chromosome content from different males and from different bundles in the same male exhibited considerable variability in mean volume (Table 1), which probably reflects systematic errors in the measurements. Since, in this study, comparisons are made within and not among bundles, absolute values of volume are not essential.

The nuclei of sperm of *Canton–S* wild-type males were used as the standard for these experiments. The quantity of chromatin was varied by utilization of an attached $XY$ chromosome, compound autosomes, or a translocation. The translocation also provided a means of varying the chromatin arrangement between centromeres while keeping the amount of chromatin constant. A pericentric inversion was used to rearrange the chromatin with respect to a single

centromere. A description of the genetic constitution employed and the rationale for each experiment are included with the results. The descriptions of the mutants and the chromosomes are given in LINDSLEY and GRELL (1968). The flies were raised at $25° \pm 2°$ in uncrowded cultures on cornmeal and molasses media.

## INFLUENCE OF CHROMOSOMAL CONTENT ON NUCLEAR DIMENSIONS

*Canton-Special*: One-half of the sperm produced by wild-type males have an $X$ chromosome and one-half have a $Y$ chromosome, whereas the autosomal complement is uniform in all the sperm. Three bundles of nuclei from two different males were sectioned. The data from one of these are summarized in Table 1, and Figures 6 and 7. They are derived from 38 scanned negatives taken over a distance of 16 $\mu$m, i.e., at approximately 0.4 $\mu$m intervals. Sixty-one nuclei were
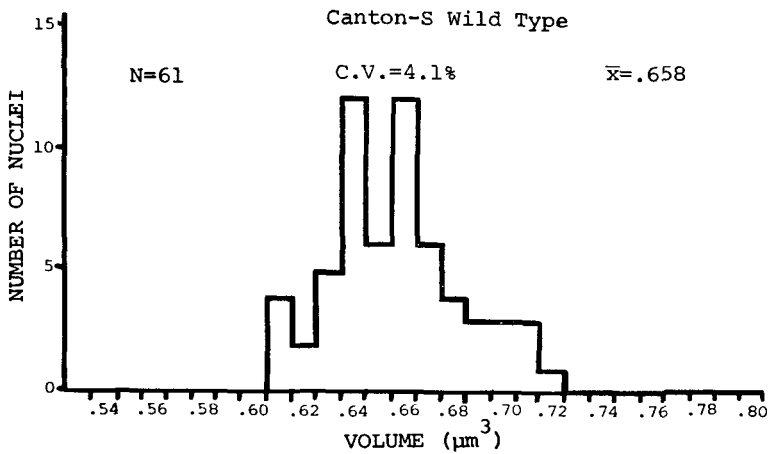


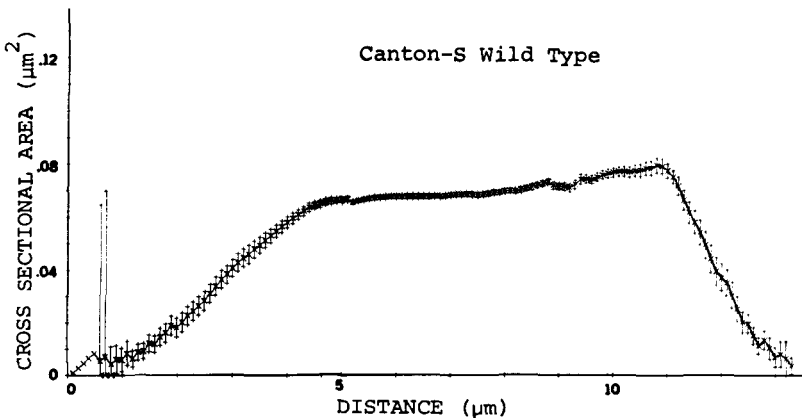FIGURE 6.—Volume distributions of nuclei in a bundle of spermatids from a Canton–S male.



FIGURE 7.—Average cross-sectional area curve of the group of nuclei seen in the volume distributions from a Canton–S male. The error bars represent the 95% confidence limits.

found in this bundle. Many authors have reported fewer than 64 spermatid tails in bundles from wild-type males. The nuclear volumes of all three bundles were normally distributed (e.g., Figure 6).

The average cross-sectional area curve and 95% confidence limits based on the variance among observed values for each point are shown in Figure 7. The limits are wider at the ends of the curve as they are derived from fewer nuclei; the points between 0.0 and 0.5 μm having no confidence limits are derived from one nucleus that extends beyond the others. Irregularities at the extremes of the curve are attributable to the fact that the averaged curves are slightly out of register. The plot is arranged so that the acrosome end is on the left and the axonemal end is on the right. The maximum of the curve corresponds approximately to the position of the centriole (See Figure 4b, PEROTTI 1969). Since the nuclear cross-sections are approximately circular, the shape of the curve indicates the nuclei are roughly cylindrical with tapering ends. They widen rapidly from the acrosome ends for about 25% of their length, more gradually for the next 60%, and then decrease abruptly for the remaining 15% of their length.

The average length of about 11 μm (Table 1) is in fair agreement with lengths reported by other authors, although estimated lengths vary considerably among bundles (Table 1). As expected from the volume distribution, the lengths of nuclei in this bundle are normally distributed.

$Y^sX \cdot Y^L$, $In(1)EN$, $\gamma$ B/O: XY/O males produce sperm having the XY chromosome plus autosomes and sperm having just the autosomes.

If the $X$ or $Y$ chromosomes are taken as equal to an autosomal arm and the autosomal arms are about equal, the ratio between the amounts of chromatin which these two sperm types contain can be estimated from the arm ratio to be about 6:4 (HERSKOWITZ and MULLER 1954), assuming that the XY chromosome contains virtually all of the $X$ and the $Y$.
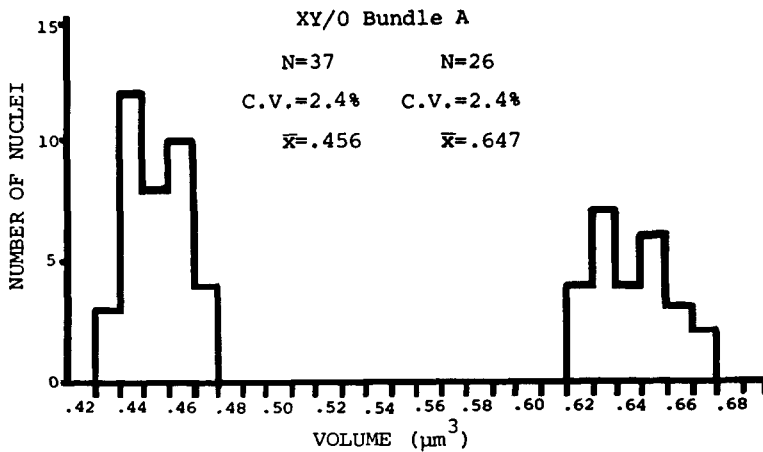


FIGURE 8.—Volume distributions of nuclei in Bundle A of spermatids from a $Y^sX \cdot Y^L$, $In(1)EN$, $\gamma$ B/O male.

Genetic crosses and examination of metaphase chromosome preparations confirmed the presence of the $XY$ and the absence of a free $Y$ chromosome in the stock from which the males examined were chosen. Three bundles of nuclei from two $XY/O$ males were sectioned. Bundles A and B were in the same male. The data from bundle A, presented in Table 1 and Figures 8 and 9, are derived from 30 scanned negatives selected from 60 pictures taken over a distance of 12.5 $\mu$m, i.e., at about 0.4 $\mu$m intervals. Although this bundle contained 64 sperm tails, there were but 63 nuclei. The data for bundle B, presented in Table 1 and Figures 10 and 11, are derived from 11 scanned negatives selected from 48 pictures over a distance of 12.3 $\mu$m, i.e., at about 0.9 $\mu$m intervals. The number of
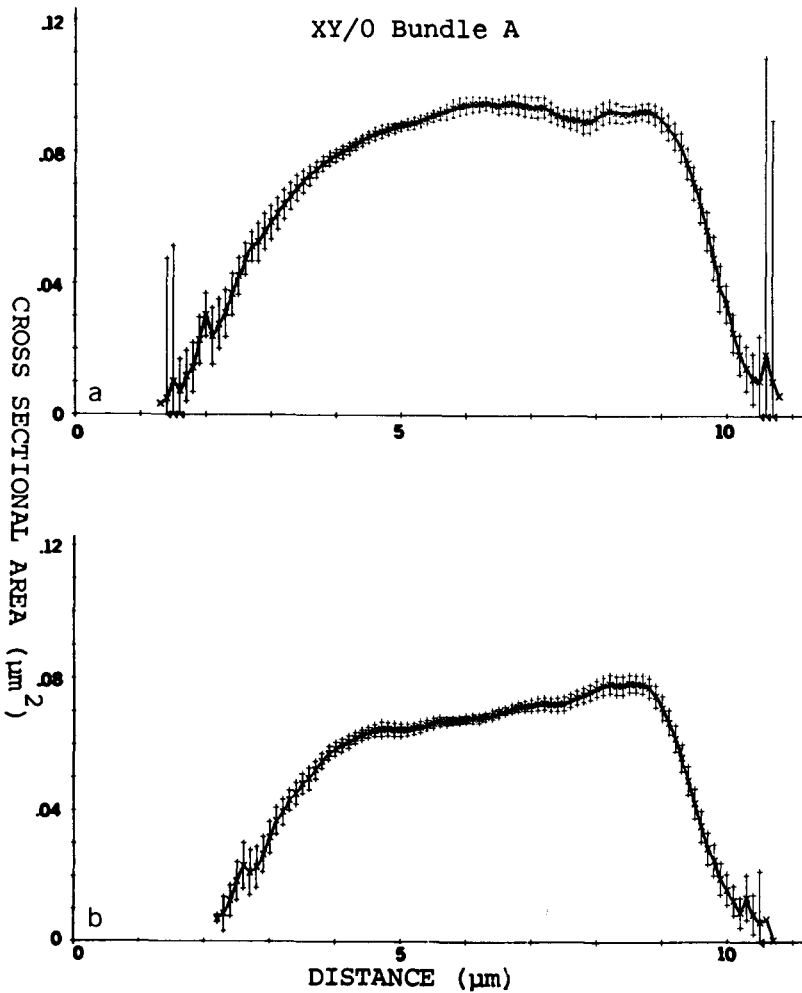


FIGURE 9.—Average cross-sectional area curves of the groups of nuclei seen in the volume distributions from $Y^SX \cdot Y^L$, $In$ $(1)EN$, $\gamma$ $B/O$ Bundle A. (a) Larger nuclei; (b) Smaller nuclei. The error bars represent the 95% confidence limits.
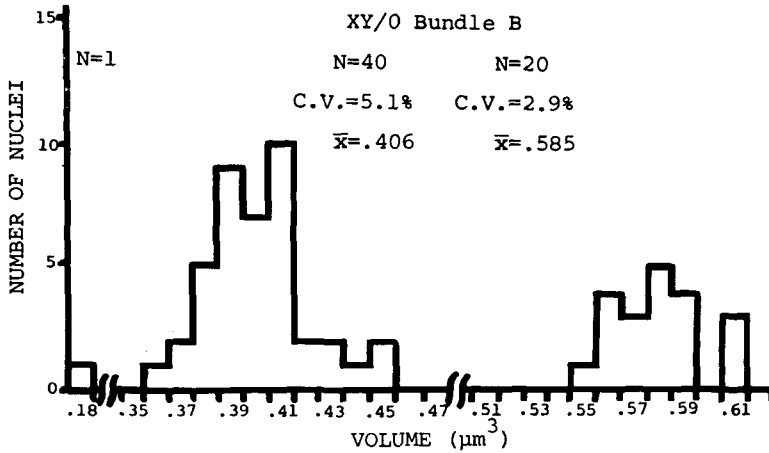
FIGURE 10.—Volume distributions of nuclei in Bundle B of spermatids from a $Y^sX \cdot Y^L$, In (1)E V, y B/O male.

scanned negatives was reduced to approximately one per μm since it was recognized empirically that the volume and cross-sectional area curves of bundle A could be practically obtained from fewer negatives.

The volume distributions for the two bundles are shown in Figures 8 and 10; they are clearly bimodal, as expected if the quantity of chromatin affects nuclear size. The groups with the larger volumes are thought to represent nuclei containing the $XY$ chromosome and the groups with the smaller voumes the nullo-$X$, nullo-$Y$ nuclei. The ratio of the mean volumes of the two groups in bundle A is 1.42, and in bundle B it is 1.44. In both bundles the number of smaller nuclei exceeds the number of larger nuclei (Table 1, Figures 8 and 10). Furthermore, the numbers of nuclei in the groups with the smaller volumes are greater than 32. This observation suggests chromosome loss from some of the nuclei.

In Figure 10, one nucleus is seen that has an appreciably smaller volume than the other nuclei. Although this nucleus does not have a tail or acrosome associated with it, its electron density is identical to that of other nuclei. The addition of its volume to the mean volume of the smaller nuclei results in a value close to the mean volume of the larger nuclei. Nuclei of such reduced dimensions are referred to as *micronuclei* and are believed to carry only the $XY$ chromosome. This finding, as well as the deviations from mendelian expectations, are discussed further in the section on micronuclei.

The cross-sectional areas curves of the two bundles are shown in Figures 9 and 11. The curves for nuclei having the larger volumes are in (a) and those for the smaller nuclei are in (b). In each figure the two curves are similar except that (a) is larger than (b) in both length and height. The mean lengths of the nuclei for the various groups are shown in Table 1. As in wild type, the nuclear length distributions agree with normality.

In addition to the two bundles reported above from one male, one bundle from a different male was analyzed. It contained 38 smaller and 25 larger nuclei; in
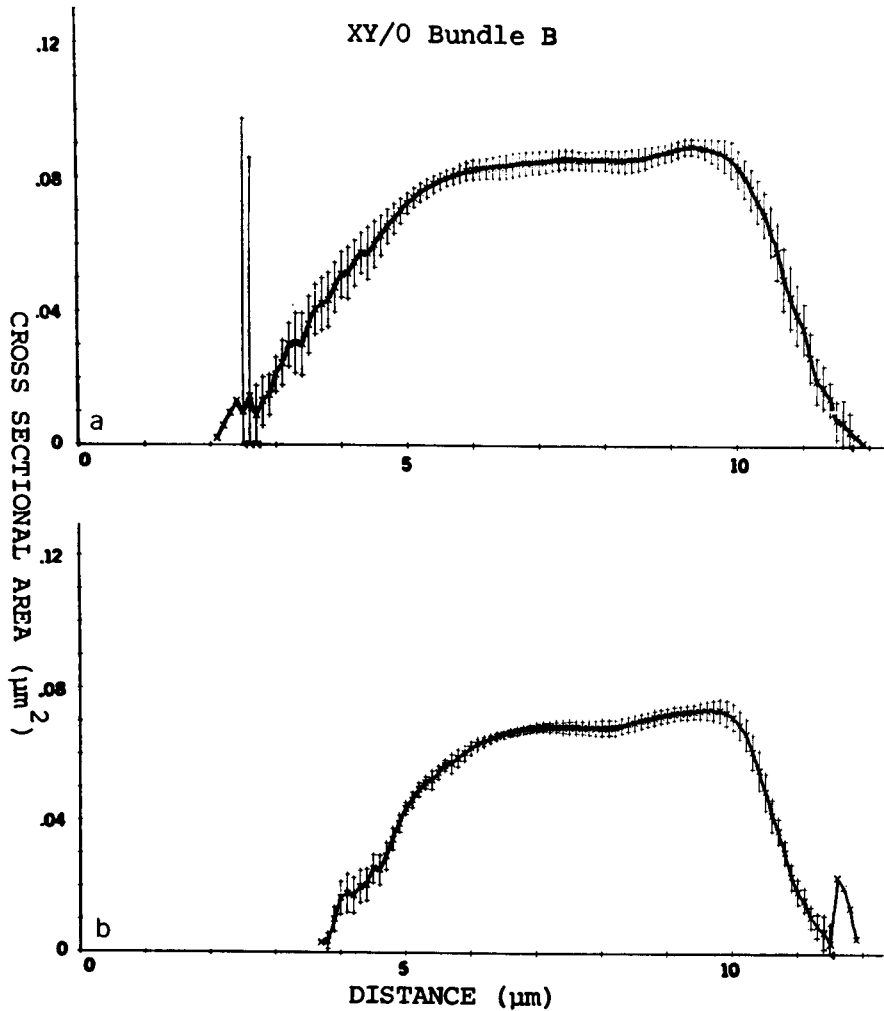
FIGURE 11.—Average cross-sectional area curves of the groups of nuclei seen in the volume distributions from $Y^S X \bullet Y^L$, *In (1)EN*, $\gamma$ *B/O* Bundle B. (a) Larger nuclei; (b) Smaller nuclei. The error bars represent the 95% confidence limits.

the cross-sections of one of the spermatids a micronucleus was seen in juxtaposition to and enclosed within the same plasma membrane as a bigger nucleus (Figure 21d).

$Y^S X \bullet Y^L$, *In(1)EN*, $\gamma$ *B/$\gamma^+$Y*: These males produce two types of sperm, those having the *XY* chromosome plus autosomes and those having the *Y* chromosome plus autosomes. The expected ratio between their volumes based on metaphase chromosome arm lengths is about 6:5, which is not as great as in *XY/O* males. This expectation is provisional because in addition to the uncertainties about the size of the attached *XY* chromosome, the $\gamma^+Y$ chromosome contains an unknown

amount of material derived from the $X$ chromosome (LINDSLEY and GRELL 1968).

The distribution of volumes is shown in Figure 12 and the cross-sectional area curves in Figure 13. These data, summarized in Table 1, are derived from 14 scanned negatives, sampled at about 0.9 $\mu$m intervals, and selected from 34 pictures taken over a distance of 14 $\mu$m along the bundle of nuclei.

Both the volume (Figure 12) and length distributions (Table 1) are bimodal with some overlap between the two groups. The groups are assigned equal numbers, as misclassification of a nucleus on the interface of the modes will change the mean volumes by less than 1%. In addition, a mass mating of 25 $XY/\gamma^+Y$ males to 50 $\gamma\ w$ females gave 984 $\gamma\ B$ females and 1025 $w$ males, indicating that the $XY$ chromosome is recovered as frequently as the $\gamma^+Y$ chromosome. The ratio of the mean volumes of the two groups is 1.12 (Table 1). Their volumes and lengths are normally distributed.

In addition there are two nuclei in Figure 12 whose volumes are significantly different from the majority, which can be explained by postulating a non-disjunction in the first meiotic division and loss of the two other nuclei having the non-disjunction and loss of two nuclei having normal disjunction products. It may be noted that the mean volume of the two exceptional nuclei is .610 $\mu$m$^3$, which coincides with the mean of the two modes. The ratio of nuclear volumes of these two disparate nuclei is 1.75 (.776/.444, see Table 1), as expected if one carries both the $XY$ and the $Y$ and the other carries neither. Hence, these data suggest that non-disjunction of the sex chromosomes occurred in the first meiotic division and further suggest preferential failure of exceptional nuclei to reach maturity.

The average area curve for the smaller nuclei is shown in Figure 13b and for the larger in Figure 13a. The average area curve for the larger nuclei is larger in all dimensions than the curve for the smaller nuclei.
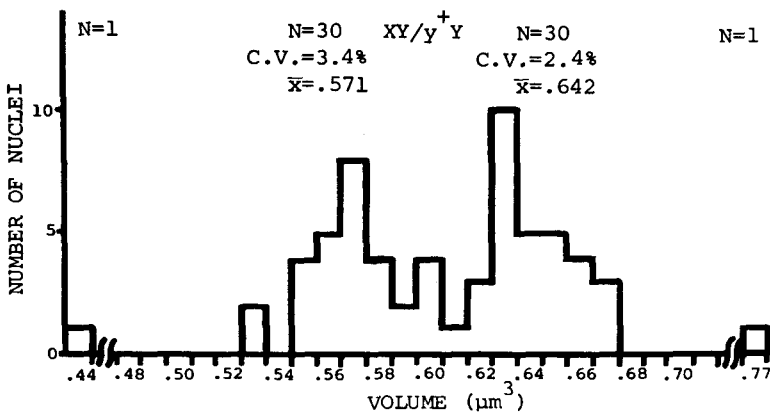


FIGURE 12.—Volume distributions of nuclei in a bundle of spermatids from a $Y^SX \bullet Y^L$, $In(1)EN, \gamma\ B/\gamma^+Y$ male.
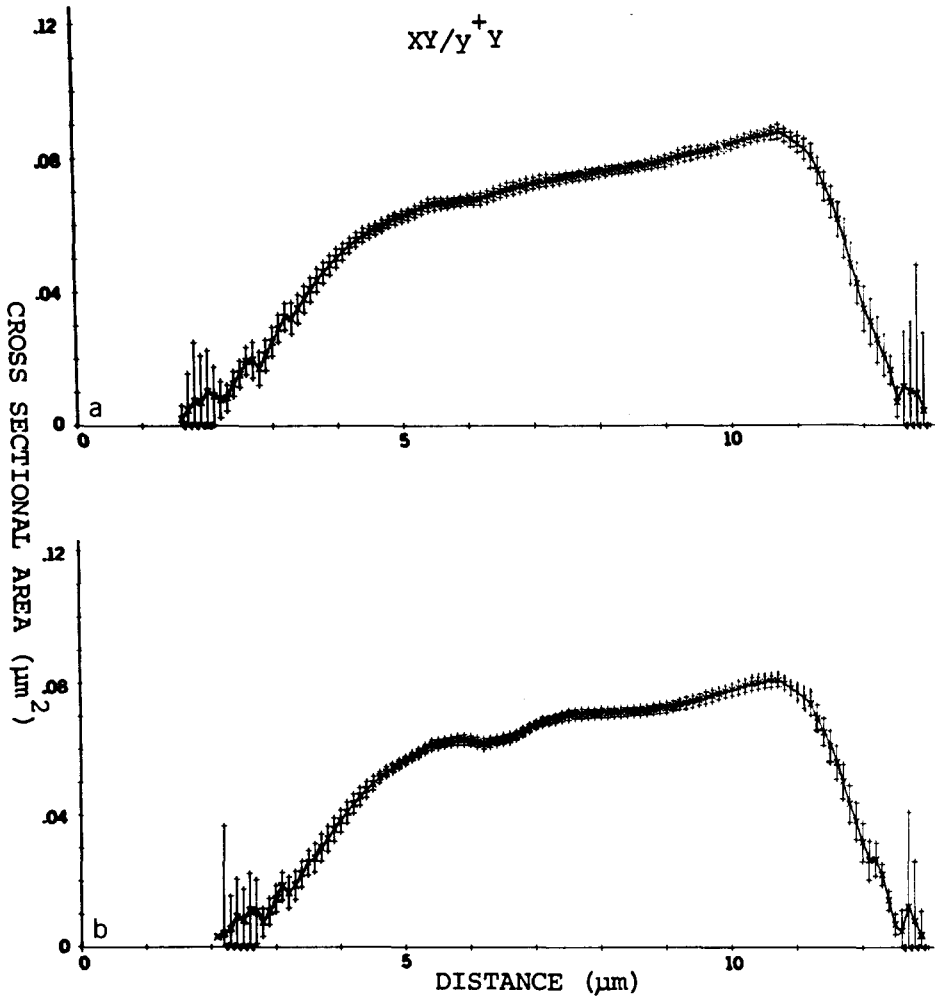
FIGURE 13.—Average cross-sectional area curves of the groups of nuclei seen in the volume distributions from a $Y^sX \cdot Y^L$, $In(1)EN$, $y$ $B/y^+Y$ male. (a) Larger nuclei; (b) Smaller nuclei. The error bars represent the 95% confidence limits.

$C(2L)RM\#4$, $dp$; $C(2R)RM\#4$, $px$: In addition to having either an $X$ or $Y$ chromosome, a sperm from this male can be nullo-$2$; diplo-$2L$, nullo-$2R$; nullo-$2L$, diplo-$2R$; or diplo-$2$. Ignoring the sex chromosome difference, which wild-type bundles show to be undetectable, the ratio of chromosomal content among the four classes of nuclei is about $7:5:5:3$. Nuclei from males of this genotype have the most extreme ratios examined in this report. In addition, the diplo-$2L$, nullo-$2R$ and nullo-$2L$, diplo-$2R$ groups are a test for a morphological effect on sperm head shape of duplicated chromosome arms when on a single centromere. It is possible that $2L \cdot 2L$- and $2R \cdot 2R$-bearing nuclei will show no difference in shape; however, if $2L$ and $2R$ occupied mutually exclusive sites, then an effect might be expected.

The data are derived from 17 scanned negatives, spaced about 1.0 $\mu$m apart, and selected from 51 pictures taken over a distance of 18 $\mu$m along the bundle of nuclei.

The volume distribution (Figure 14) is trimodal, as is the head length distribution (Table 1). The volume distribution of the middle group is not significantly different from a normal distribution. The number of nuclei in the middle group (35) should be binomially distributed and can exceed 32/64 since in males the two attached chromosomes segregate independently. On mendelian grounds the numbers of nuclei in the extreme modes should be equal, since they contain reciprocal products of the same meioses; however, there are 15 small and 8 large nuclei. Assuming that all six nuclei missing from this bundle of 58 were lost from the large class does not restore equality. A possible explanation is discussed in the section on micronuclei.

The cross-sectional area curves of the larger, intermediate, and smaller volume groups are shown in Figures 15a, b, and c, respectively. The narrower 95% confidence limits seen in the middle curve reflect the greater number of nuclei in this group. The curves are generally similar to the wild-type curve.

$In(3LR)C269/+$: The pericentric inversion is homozygous viable and has breakpoints on the salivary chromosome map at 78C and 98F. It places almost all of the euchromatin of the third chromosome on one side of the centromere (LINDSLEY and GRELL 1968).

These males produce four kinds of sperm since they are heterozygous for the sex and inverted third chromosome. The volume of sperm nuclei having the inversion is not expected to differ from those with a normal third chromosome. However, if centromeres and arms occupy specific sites within the spermatid nucleus during condensation, then the morphological effect of the inversion might be seen in the cross-sectional area curves.
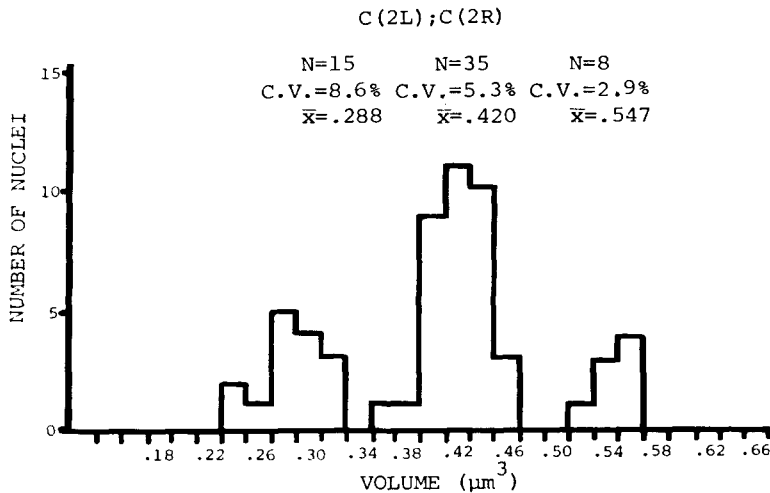
C(2L);C(2R)



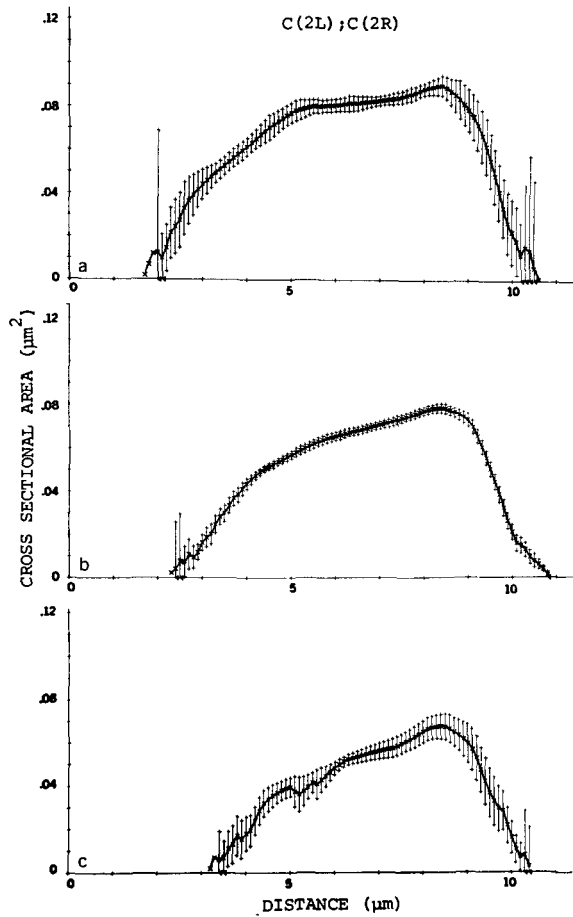FIGURE 14.—Volume distributions of nuclei in a bundle of spermatids from a C(2L)RM#4, dp; C(2R)RM#4, px male.

FIGURE 15.—Average cross-sectional area curves of the groups of nuclei seen in the volume distributions from a *C(2L)RM#4, dp; C(2R)RM#4, px* male. (a) Larger nuclei; (b) Intermediate nuclei; (c) Smaller nuclei. The error bars represent the 95% confidence limits.

The data summarized in Table 1 and Figures 16 and 17 are derived from 12 scanned negatives spaced about 0.86 $\mu$m apart. They were selected from 39 pictures over a bundle distance of 12.2 $\mu$m.

The volume (Figure 16) and head length distributions are unimodal and don't differ significantly from normality.

The cross-sectional area curve and its 95% confidence limits are shown in Figure 17. The curve flattens more than the wild type but the 95% confidence limits are very narrow, suggesting little if any difference in morphology of the nuclei. This curve is taken to be the most representative of the true cross-sectional areas, as the bundle has the least deviation from the perpendicular to the cutting direction, i.e., the smallest angle $\theta$.

*T(2;3)lt^{m7}/+*: The translocation break points are at 40B-F and 100F on the
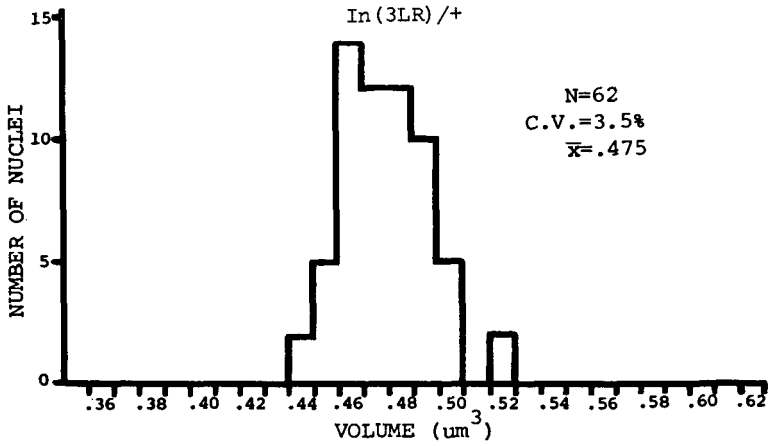
FIGURE 16.—Volume distributions of nuclei in a bundle of spermatids from a *In(3LR)C269/+* male.
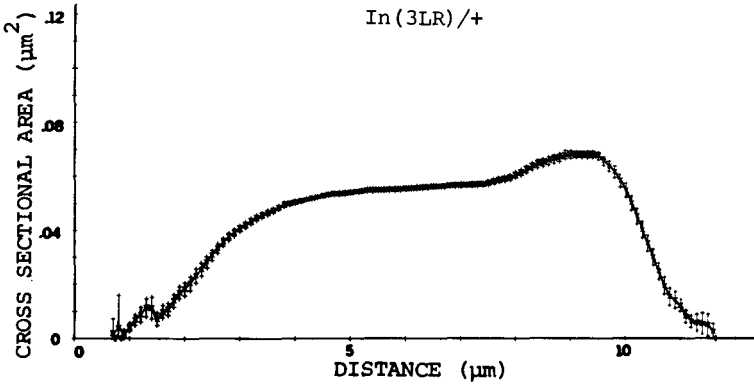


FIGURE 17.—Average cross-sectional area curves of the groups of nuclei seen in the volume distributions from a *In(3LR)C269/+* male. The error bars represent the 95% confidence limits.
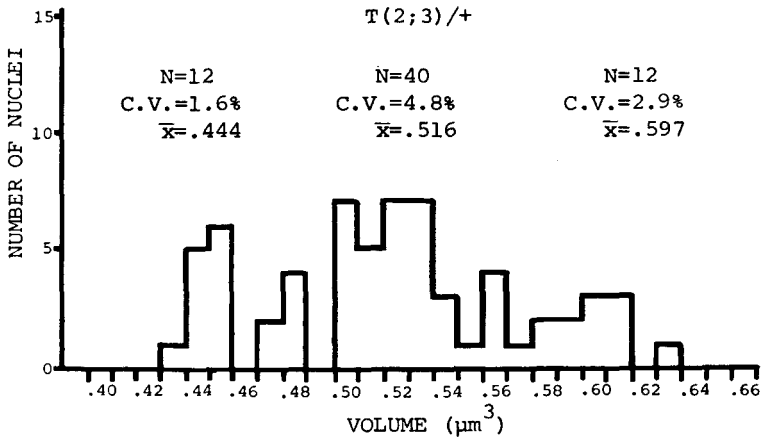


FIGURE 18.—Volume distributions of nuclei in a bundle of spermatids from a *T(2;3)lt^{mr}/+* male.

salivary chromosome map and append the entire left arm of the second chromosome onto the tip of the right arm of the third chromosome.

Disregarding the sex chromosomes, these males commonly produce four types of sperm. Alternate disjunction leads to sperm with five chromosome arms, whereas both types of adjacent segregation lead to equal numbers of products with four and six arms; thus expected DNA ratios are about 6:5:5:4. Rare three to one segregations of the translocation elements may give two additional classes of ratio 7:3. Among the balanced gametes, i.e., the largest class, the volume distribution is expected to be similar to wild type. However, a morphological effect caused by the translocation of chromatin beween chromosomes could appear in the cross-sectional area curves.

The data are summarized in Table 1 and Figures 18 and 19. They are derived from 22 scanned negatives at 0.56 μm intervals, over a distance of 13 μm along the bundle. The male was crossed to test for the presence of the translocation before dissection.

The distribution of volumes (Figure 18) and head lengths (Table 1) are trimodal, with some overlap between the groups. The overlap may be explained
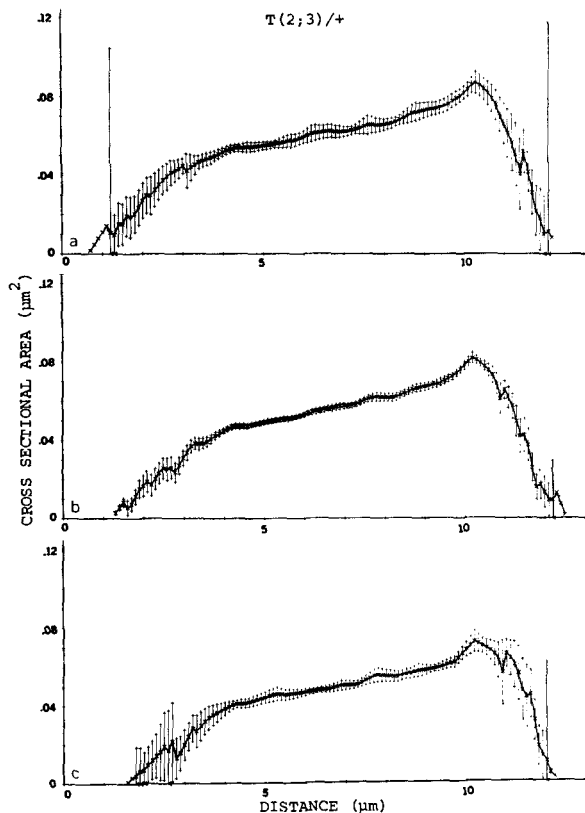


FIGURE 19.—Average cross-sectional area curves of the groups of nuclei seen in the volume distributions from a $T(2;3)lt^{m7}/+$ male. (a) Larger nuclei; (b) Intermediate nuclei; (c) Smaller nuclei. The error bars represent the 95% confidence limits.

by the finding that $\theta$, the tilt of the bundle, changed from about 9° at the axonemal end to about 19° at the acrosomal end. This was the largest $\theta$ found. The groups with the small and large volumes were assigned 12 members each by inspection—10 alternate and 6 adjacent disjunctions. The distribution of the middle group appears to be normal.

The cross-sectional area curves are shown in Figure 19. One-half the nuclei in Figure 19b have the translocation and the other half have a normal complement. The sex chromosomes are distributed at random among these. Figures 19a and 19c are derived from the group of nuclei with the larger and smaller mean volumes, respectively, in Figure 18.

## MICRONUCLEI

In three sperm bundles from $XY/O$ males 186 of the possible 192 sperm were measured. The loss of a few sperm from a bundle of 64 is not unusual, as mentioned before. If meiosis were normal, 96 of the 192 sperm should have carried an $XY$ chromosome; however, only 71 nuclei were of such a volume as to indicate that they carried an $XY$ chromosome, and the remainder were of a volume expected for nullo-$X$, nullo-$Y$ nuclei. Thus, even assuming that the six nuclei missing from the three bundles carried an $XY$ chromosome, there is a discrepancy of at least 19 $XY$-bearing nuclei, and a corresponding excess of nullo-$X$, nullo-$Y$ nuclei. These observations are interpreted as showing that a fraction of the $XY$-bearing nuclei are converted to nullo-$X$, nullo-$Y$ nuclei by loss of the $XY$ chromosome. Furthermore, in genetic crosses of $XY/O$ males the recovery of the $XY$ chromosome is commonly less than expected. For instance, twenty-five 3-day-old males that were brothers of those dissected for the volume measurements were mass-mated to 50 wild-type females. After 3 days the parents were transferred and 4 days later they were discarded. The progeny comprised 709 females and 1139 males. The ratio of males to females was 1.61 (1139/709), compared with 1.62 (115/71) for the nuclear volume data. The identity of these ratios may have been fortuitous, as the final ratio of the $XY$ chromosome in progenies seems to depend on the length of time the females are allowed to produce (OLIVIERI and TANZARELLA 1973). In $XY/Y$ males, on the other hand, equal numbers of the two classes of spermatid nuclei are observed, and micronuclei are absent; furthermore, their progenies exhibit a sex ratio of unity. The segregation of the $XY$ chromosome into a micronucleus in a fraction of the $XY$-bearing spermatids and the subsequent loss of micronuclei in the $XY/O$ but not $XY/Y$ males accounts for both the measured ratios of nuclear volumes and the observed sex ratios.

A preliminary search for evidence of abnormal chromosome behavior during meiosis was carried out. Testes from pupae and young males were dissected in saline, placed in aceto-orcein stain, and squashed before observation using phase optics. Meiosis appeared normal; the few second-anaphase divisions that were scored showed a completely normal chromosome complement. This observation, coupled with the finding of micronuclei in post-individualization spermatid bundles in $XY/O$ testes, suggests that micronuclei are formed during spermio-
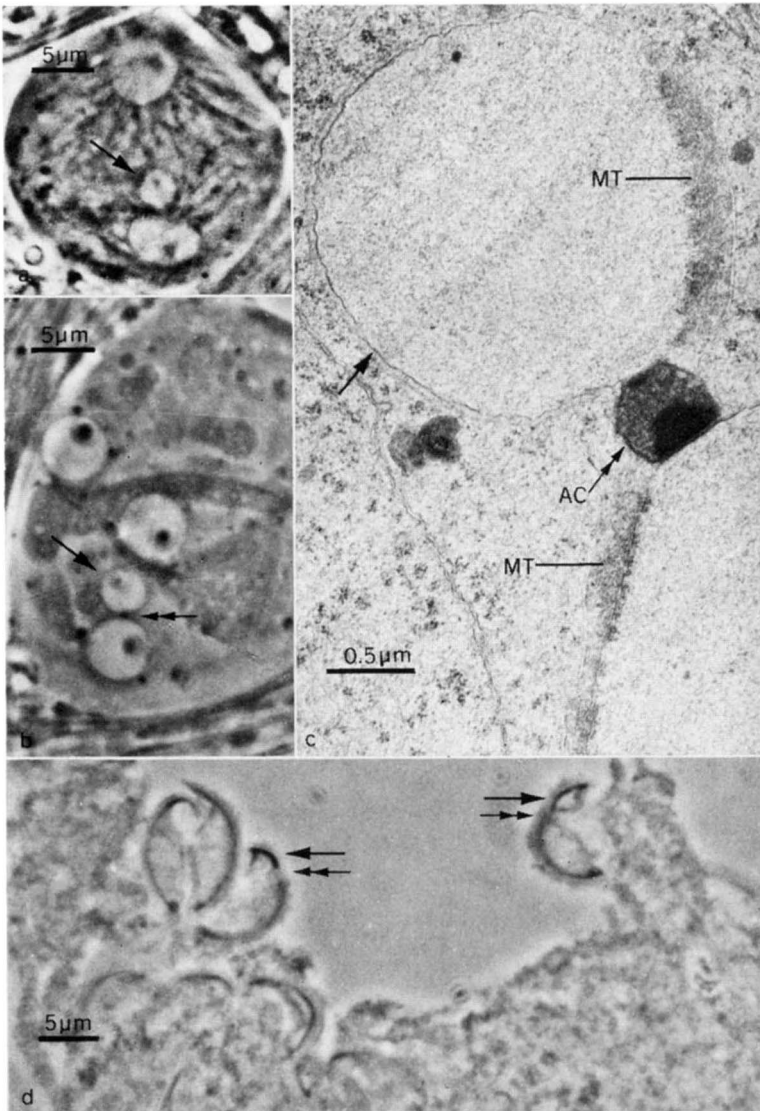
FIGURE 20.—Light and electron micrographs of spermatid nuclei in various stages of development. (a) Light micrograph of two spermatids just after the second meiotic division. One spermatid is binucleated. The arrow points to the micronucleus. Aceto-orcein stained squash preparation, phase optics. (b) Light micrograph showing several spermatid nuclei in a more advanced stage than in (a). One of the spermatids has a micronucleus (arrow). The dark granule seen between the two nuclei is the acrosome. Saline squash, phase optics. (c) Electron micrograph of a binucleate spermatid in the same developmental stage as in (b). The micronucleus (arrow) is connected to the macronucleus by the acrosome (AC and double-headed arrow). A bundle of microtubules, MT, is forming in association with each nucleus. The bundles may be on opposite sides of the acrosome as in (c) or on the same side. (d) Light micrograph of spermatids in a later stage than seen in (b). The large arrows point to two micronuclei and the double-headed arrows to the presumptive acrosomal regions. Normal-appearing spermatid nuclei are also seen. Aceto-orcein stained squash preparation, phase optics.

genesis. In fact, micronuclei were first observed immediately following the second meiotic division. This is illustrated in Figure 20a, which is a light micrograph of two newly-formed spermatids. One has two nuclei, one of which appears to be a micronucleus. Aceto-orcein staining indicates that such a nucleus contains stainable material.

Micronuclei can be observed to persist through later stages of spermiogenesis. Figure 20b shows three very young spermatids, one of which has two nuclei of different sizes connected by a dark granule. An electron micrograph of a cross-section through nuclei in a similar stage of development shows the dark granule to be the developing acrosome (Figure 20c). Serial sections of these nuclei confirm the absence of another acrosomal body. The significance of this association is not known; when both nuclei have begun to elongate they are still conjoined end-to-end by the acrosomal primordium (Figure 20d). The spherical, amorphic, electron-dense body seen transiently in the nuclei of young spermatids of both normal and $XY/O$ males (TATES 1971) is also seen in the micronucleus (Figure 20b).

A bimodality of nuclear volumes is already apparent at the time of full spermatid elongation ($L$ and $S$ in Figure 21a). In addition, spermatids were found that show two nuclear profiles in cross-section. The larger of the two nuclei, the macronucleus, has approximately the same volume as those in the smaller class.

The development of micronuclei parallels that of macronuclei. The nuclear pores (fenestrated membrane) of each faces inwardly adjoining the bundle of microtubules found in the concavity of the macronucleus; a single layer of microtubules becomes associated with the outer convex surface of each; and the migration of the two paranuclear structures described by TOKUYASU (1974) takes place in both.

TOKUYASU (1974) showed that the paranuclear structures traverse the length of the nucleus along the surface of the nuclear envelope and that the nucleus becomes deeply indented at the site of the major paranuclear structure at its acrosomal end (small arrows in Figure 21a). With the degree of indentation as a structural marker, the acrosomal end of the micronucleus can be identified. Analysis of several micronuclei in the bundle shown in Figure 21a reveals that a micronucleus may be associated with a macronucleus in several ways. Their acrosomal ends may be pointed in opposite directions, either both associated with the acrosome (Figure 20d) or with the macronucleus associated with the acrosome and the micronucleus offset and shifted toward the base of the macronucleus. Alternatively, the acrosomal ends may be pointed in the same direction and the two nuclei arranged in parallel (Figure 21a); in such cases the acrosome is also associated with the macronucleus.

The latest stage of spermiogenesis at which micronuclei have been seen in the light microscope is shown in Figure 21b. Sixty-three nuclei, about 6 $\mu$m long, are seen in this bundle along with 6 shorter micronuclei. The excess over 64 agrees with the supposition that the micronuclei are derived from the same meiotic product as macronuclei. Just prior to individualization the micronucleus appears to contain condensed chromatin (Figure 21c).
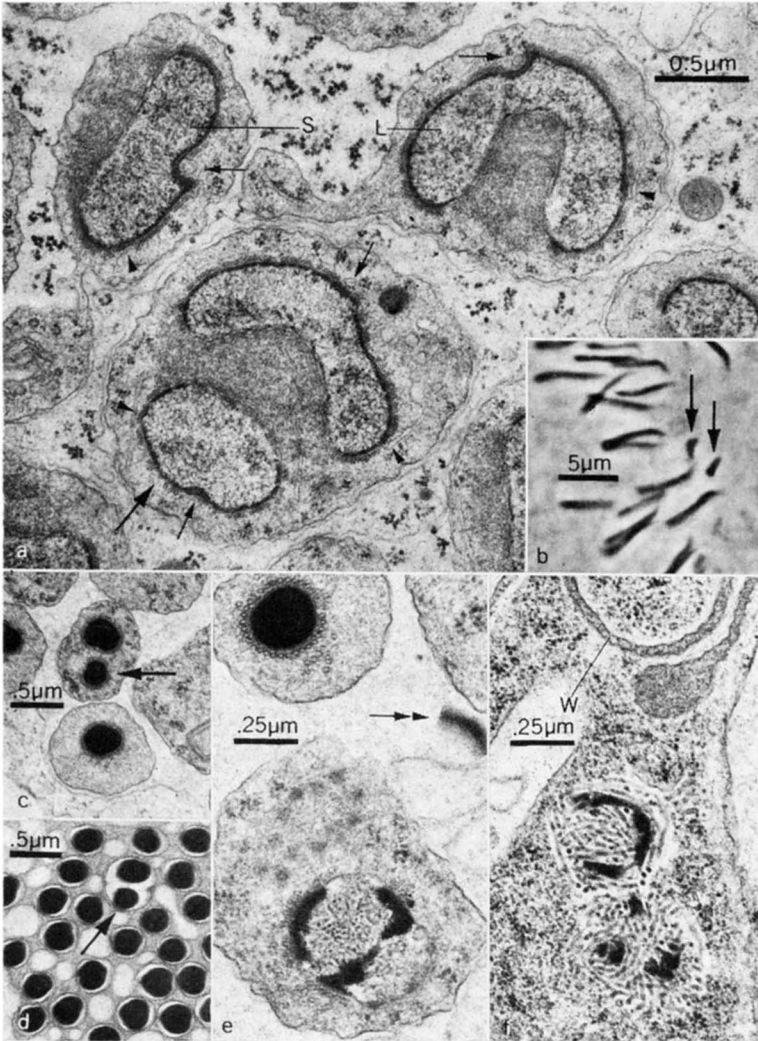
FIGURE 21.—Spermatid nuclei in various stages of development. (a) Electron micrograph showing cross-sections of the nuclear regions of three spermatids in a similar stage of development to those in Figure 20d. The largest arrow points to the micronucleus of a binucleate spermatid. The small arrows point to the major perinuclear structures and the arrow heads to the minor perinuclear structures. L, larger-volumed nucleus; S, smaller-volumed nucleus. (b) Light micrograph of spermatids in a later stage than in (a). The arrows point to two micronuclei. (c) Electron micrograph of cross-sections of spermatid nuclei just prior to individualization as shown by the arrangement of microtubules around each nucleus. The arrow points to the micronucleus of a binucleate spermatid. (d) Spermatid nuclei in the early coiling stage. The arrow points to the micronucleus of a binucleate spermatid. (e) Abnormal-appearing nucleus just prior to individualization. The double-headed arrow indicates an acrosome. A normal-appearing nucleus is in the top of the figure. (f) A portion of a waste bag containing two abnormal nuclei along with other detritus. The nuclei appear to have begun degeneration as the thread-like structures in these nuclei are thicker than those in (e). W, mitochrondrial whorl commonly seen in waste bags.

In the bundles that were serially sectioned, one micronucleus was found in each of two $XY/O$ post-individualization bundles (e.g., Figure 21d); however, in the bundle of spermatids sectioned in a stage prior to individualization at least five micronuclei were seen (Figure 21a). This observation suggests that the micronuclei formed during meiosis are later removed, probably by the individualization process (TOKUYASU, PEACOCK and HARDY 1972a) as it traverses the nuclei. The micronuclei in the later stages are less than 0.2 $\mu$m wide and 2 $\mu$m long; hence, identification in the light microscope is very difficult. Figure 21e is an electron micrograph of a cross-section of a pre-individualization spermatid nucleus having an abnormal appearance. The finding of similar nucleus-like structures in the accumulations of debris formed during the individualization process (compare Figures 21e and 21f) supports the above supposition. Nevertheless, the fate of micronuclei has not been rigorously determined.

The explanation proposed for the concordance of the numbers of nuclei with large and small volumes with the sex ratio in the progenies of $XY/O$ males predicts the incidence of micronuclei in young spermatids. To check this prediction eleven three-day-old males were placed singly in vials with two virgin $y$ $w$ free-X females. After mating for three days the males were removed and dissected. The females were brooded through five more three-day intervals. The testes of the parental males were examined in saline preparations and the number of micronuclei in the stage shown in Figure 20b was scored. Of 994 spermatids, 83 had a micronucleus. The ratio of males to females expected in the progenies based on these figures is 1.40 $[(994 \times .5 + 83)/(994 \times .5 - 83)]$, which, considering the uncertainty in scoring micronuclei, is close to the small:large nuclear ratio of 1.62 (115/71) and the male to female progeny ratio of 1.59 (1728/1087; Table 2). In addition, it was noted the sex ratio in the progenies of the males increased in later broods (Table 2). Had the females been brooded until they exhausted their sperm supply, the overall sex ratio might have been slightly greater.

In one bundle sectioned just prior to individualization several binucleate spermatids were observed to have abnormally condensed macronuclei. No trace of such nuclei was observed in the three post-individualization bundles examined. Such abnormal nuclei may, therefore, be eliminated during individualization (i.e., 186/192 nuclei survived individualization). Even though nuclei persisting past individualization are normally condensed, the fact that younger spermatids

TABLE 2

*Progenies from crosses of single* $Y^SX \bullet Y^L$, In(1)EN, y B/O *males to two* y w *females*

The males were removed after three days and the females transferred to new vials at three-day intervals until 18 days after insemination had elapsed.

| 11 Males | Days | 1–3 | 4–6 | 7–9 | 10–12 | 13–15 | 16–18 | Total |
|---|---|---|---|---|---|---|---|---|
| | Males | 202 | 162 | 290 | 347 | 336 | 391 | 1728 |
| | Females | 204 | 157 | 186 | 226 | 151 | 163 | 1087 |
| Ratio $\dfrac{\text{Males}}{\text{Females}}$ | | .99 | 1.03 | 1.56 | 1.54 | 2.22 | 2.40 | 1.59 |

were found in which the acrosome was not at its normal terminal location, but at the junction between the micronucleus and macronucleus (Figure 20), suggested that in later stages some acrosomal abnormalities would be observed. The *XY/O* bundle whose data are not in this report had two spermatids with the larger nuclei whose acrosomes were displaced caudally about $\frac{1}{3}$ the distance toward the axoneme. In the same bundle two of the smaller nuclei had no visible acrosomes. In bundles A and B of the *XY/O* in this report, one spermatid missing an acrosome was found in each. Assuming none of these forms, functional sperm does not change the nuclear ratio significantly. The presence in the coiling stage of sperm having smaller nuclei without an acrosome suggests the hypothesis that removal of the micronucleus occurs during individualization, and the acrosome being associated with both nuclei is sometimes removed as well.

The spermatids of *C(2L)*; *C(2R)*-bearing males also contained micronuclei. The observed inequality of reciprocal classes (Figure 14) may have an explanation similar to that of the *XY/O* males; i.e., micronuclei containing a compound autosome are generated during the meiotic divisions and later removed during individualization. The consequences of such an occurrence, unlike in the *XY/O* males where an *XY* nucleus is converted into a nullo-*X*, nullo-*Y* nucleus, are more complicated. Diplo-*2* nuclei may be converted to diplo-*2L*, nullo-*2R*; to nullo-*2L*, diplo-*2R*; or to nullo-*2* nuclei, and diplo-*2L* or diplo-*2R* nuclei may become nullo-*2*.

Males homozygous for *mei-S332*, a meiotic mutant that leads to precocious sister centromere separation and a consequent high rate of non-disjunction in the second meiotic division (DAVIS 1971), exhibit micronuclei of various sizes in developing spermatids. Micronuclei have also been observed in other compound autosome-bearing males, specifically (1) *C(3L)RM, se h rs²; C(3R)RM, sbd gl e⁸* and (2) *y²/BˢY; C(2L)RM, dp; C(2R)RM, px; C(3L)RM, h²; C(3R)RM, +*.

<div align="center">DISCUSSION</div>

*Effect of chromatin content on nuclear size and shape*: Using $1.08 \times 10^{11}$ daltons (RASCH, BARR and RASCH 1971) as the quantity of DNA in a sperm, 0.5 $\mu m^3$ as an estimate of nuclear volume, and 0.543 cc/gm as the partial volume of DNA (COHEN and EISENBERG 1968) yields an estimate of 18% as the fraction of the nuclear volume occupied by the DNA. Thus a sperm nucleus must contain a large amount of material other than DNA.

*Drosophila melanogaster* sperm heads may contain different amounts of chromosome material depending on the genetic constitution of the male. The present estimates of the volumes of sperm heads made from serial sections reveal that nuclear volume is proportional to chromosome content and inferentially to the quantity of DNA. Thus, for example, *XY*-bearing nuclei are 43% larger than nullo-*X*, nullo-*Y* nuclei and 12% larger than *Y*-bearing nuclei. *X*- and *Y*-bearing nuclei, on the other hand, appear to have comparable volumes. An estimate of the expected ratio of the volumes of *X*-bearing and *Y*-bearing sperm was com-

puted in the following way: From the ratios of the volumes of the large to the small heads in $XY/O$ (1.43) and $XY/\gamma^+Y$ (1.12), the ratio between the volumes of $\gamma^+Y$-bearing and nullo-$X$, nullo-$Y$ sperm was estimated to be 1.28 (1.43 ÷ 1.12). The DNA content of the $Y$ chromosome has not been reported, but RUDKIN (1965) estimates, based on ultra-violet absorbance measurements, that the autosomes contain 77% of the DNA of an $X$-bearing haploid complement. Thus, assuming sperm head volume to be proportional to DNA content, we estimate that the ratio between the volumes of $X$-bearing sperm and nullo-$X$, nullo-$Y$ sperm to be 1.30 (1.00 ÷ 0.77). The agreement of the two values corresponds to sperm head volumes in wild-type males (Figure 6).

The normalized curves in Figures 22 and 23 were derived by summing the area values at 10% increments along the nuclear length and dividing each sum by the grand total. The differences between curves from sperm having different genetic constitutions within an experiment is about the same as that between sperm of the same genetic constitution in different experiments. The similarity of the curves suggests that the inclusion of different amounts of chromosomes or rearranged chromosomes in sperm nuclei are not reflected as changes in nuclear
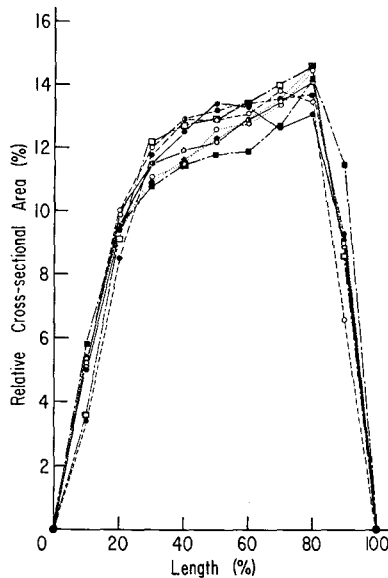


FIGURE 22.—Curves normalized to unity volume were derived by dividing the sum of the cross-sectional areas at *each* 10% increment of nuclear length by the sum of the cross-sectional areas at *all* 10% increments of length.

$XY$ nuclei from $Y^SX \bullet Y^L$, *In(1)EN*, $\gamma$ $B/O$ male Bundle A    ———●

$XY$ nuclei from $Y^SX \bullet Y^L$, *In(1)EN*, $\gamma$ $B/O$ male Bundle B    – – – –●

$O$ nuclei from $Y^SX \bullet Y^L$, *In(1)EN*, $\gamma$ $B/O$ male Bundle A    ———○

$O$ nuclei from $Y^SX \bullet Y^L$, *In(1)EN*, $\gamma$ $B/O$ male Bundle B    – – – –○

$XY$ nuclei from $Y^SX \bullet Y^L$, *In(1)EN*, $\gamma$ $B/\gamma^+Y$ male    . . . .●

$\gamma^+Y$ nuclei from $Y^SX \bullet Y^L$, *In(1)EN*, $\gamma$ $B/\gamma^+Y$ male    . . . .○

All nuclei from Canton-Special male    —.—.□

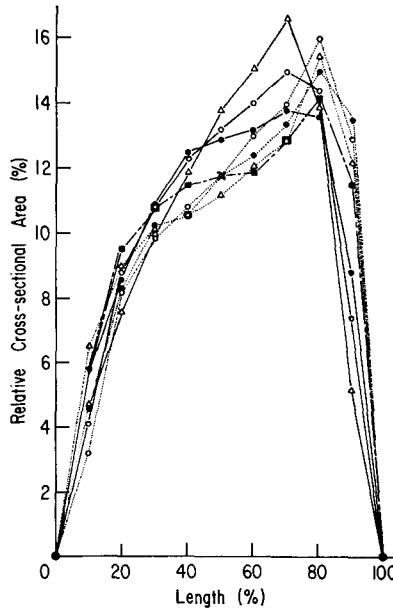All nuclei from *In(3LR)C269/*+ male    —.—.■
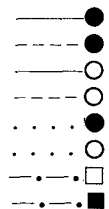
FIGURE 23.—Curves normalized to unity volume were derived by dividing the sum of the cross-sectional areas at *each* 10% increment of nuclear length by the sum of the cross-sectional areas at *all* 10% increments of length.

Large nuclei from $C(2L)RM\#4$, $dp$; $C(2R)RM\#4$, $px$ male          ———●

Intermediate nuclei from $C(2L)RM\#4$, $dp$; $C(2R)RM\#4$, $px$ male          ———○

Small nuclei from $C(2L)RM\#4$, $dp$; $C(2R)RM\#4$, $px$ male          ———△

Large nuclei from $T(2;3)lt^{m7}/+$ male          . . . . ●

Intermediate nuclei from $T(2;3)lt^{m7}/+$ male          . . . . ○

Small nuclei from $T(2;3)lt^{m7}/+$ male          . . . . △

All nuclei from $In(3LR)C269/+$ male          —.—.■
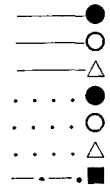
shape and supports the assumption of HERSKOWITZ and MULLER (1954) that the two kinds of sperm from $XY/O$ males ". . . had the same shape . . ."

This apparent similarity of nuclear shape bears on arguments concerning the mechanism of determining sperm head morphology. The shape of the sperm head could be determined by external molding forces such as possibly exerted by microtubules (McINTOSH and PORTER 1967). FAWCETT, ANDERSON and PHILLIPS (1971), on the other hand, argued against external molding forces on the basis of observing cases in which the pattern of chromatin condensation is apparently unrelated to the arrangement of perinuclear microtubules and postulated that a ". . . genetically controlled pattern of aggregation of molecular subunits of DNA and protein during condensation of the chromatin . . ." determines the ultimate shape of the sperm head. Recently TOKUYASU (1974) pointed out that the arrangement of perinuclear microtubules is often highly species-specific and proposed a model in which microtubules play a major role in the morpholological transformation of spermatid nuclei. He observed in *Drosophila melanogaster* that the arrangement of the microtubules is closely related to the nuclear shape and the pattern of chromatin condensation in the nucleus and

concluded that the final shape of the sperm head depends upon an interaction of nuclear constituents and cytoplasmic organelles rather than one acting independently of the other.

It is difficult to reconcile a decisive role of the chromosome condensation pattern in determination of sperm head shape with two observations: On the one hand, the chromosomal constitution of spermatid nuclei can be varied over a wide range without appreciably altering head shape. Conversely, abnormal head shapes may be observed in sperm with normal chromosomal constitutions. LINDSLEY, EDINGTON and VON HALLE (1960) observed that males carrying translocations between the $X$ and either chromosome *two* or *three* exhibit condensation of nuclear contents, but the heads are spherical or ellipsoidal rather than the elongated cylinders normally observed. It should be noted that a fraction of these abnormal heads are expected to carry a $Y$ chromosome and a normal autosomal complement. SHOUP (1967) investigated the fine structure of the spermatids produced by males carrying an $X$-$2$ translocation; she observed spermatid nuclei lacking the bundle of microtubules normally associated with the elongating nucleus. These observations fail to support an intrinsic pattern of chromosome condensation as determining head shape and are consistent with the important role assigned to perinuclear microtubules in sperm head morphogenesis by TOKUYASU (1974) .

*The change of genetic ratios with time after insemination*: A change in sex ratio among the zygotes produced by females at successive times after insemination by $XY/O$ males was previously observed by OLIVIERI and TANZARELLA (1973). Two classes of bias that may cause progeny ratios to depart from the gametic ratios can be distinguished. Preferential departure from the storage organs continuously changes the composition of the residual population of gametes in the storage organs, leading to a shift in progeny ratios with time. Once the storage organs are emptied, however, the total progeny ratio will reflect the ratio of stored gametes. Preferential transmission from the male to the female, storage, or fertilization, on the other hand, will not result in a continuously changing composition of the residual pool of stored gametes, but it will result in a progeny ratio that differs from the ratio of gametes present in the testis.

The data in Table 2, as well as those of OLIVIERI and TANZARELLA (1973), demonstrate a clear shift in the sex ratio with time as expected if $XY$-bearing sperm were leaving the storage organs preferentially. Furthermore, the overall sex ratio agrees very well with the observed ratio of large to small heads in the testis, suggesting that there is no bias in either transmission, storage, or in fertilization. Preliminary calculations indicate that $XY$-bearing sperm are 1.5 times more likely to leave the storage organs than nullo-$X$, nullo-$Y$ sperm.

*The unequal recovery of reciprocal meiotic products*: Meiotic chromosome loss in *Drosophila melanogaster* males was thought by early investigators to be the explanation for the observation that reciprocal meiotic products are not recovered equally in the progenies of males having the $sc^4sc^8$ $X$ chromosome and a normal $Y$ chromosome (GERSHENSON 1933; SANDLER and BRAVER 1954) and in males having an attached $XY$ chromosome and no free $Y$ chromosome (SANDLER and BRAVER 1954). This loss was presumed to take place during meiosis but an in-

tensive cytological search for meiotic chromosome loss (PEACOCK 1965) was negative. Furthermore, NOVITSKI and SANDLER (1957) and LINDSLEY and SANDLER (1958) observed unequal recovery of reciprocal meiotic products in cases where there was no zygote mortality and no gametes produced from which a chromosome had been lost. They were led to postulate dysfunction of certain classes of sperm.

Sperm dysfunction was reintroduced by HARTL, HIRAIZUMI and CROW (1967) and by NICOLETTI, TRIPPA and DeMARCO (1967) to explain the phenomenon of segregation distortion. Electron microscope observations by NICOLETTI (1968) and by PEACOCK, TOKUYASU and HARDY (1972) revealed that the development of up to half of the spermatids is arrested in $SD/+$ males. These observations led PEACOCK and MIKLOS (1973) to speculate that sperm dysfunction may be found in other systems such as $In(1)sc^{4L}sc^{8R}/Y$ and $XY/O$. Recently PEACOCK, MIKLOS and GOODCHILD (1974) reported that in $In(1)sc^{4L}sc^{8R}$-bearing males a fraction of the spermatids fail to become individualized and are subsequently left behind in the testes to degenerate. The fraction of spermatids that undergo such dysfunction is positively correlated with the amount of non-disjunction and meiotic drive that occurs in the male.

Turning attention to the $XY/O$ system, a search for evidence of an amount of sperm dysfunction greater than seen in wild-type males was negative except for the infrequent acrosomal abnormalities which are probably formed concomitantly with micronuclei. In addition, the inequality in the sex ratio in the progeny of this kind of male is not accounted for by invoking zygotic mortality. Single $\gamma$ $w$ females, after insemination by single attached-$XY/O$ males, were transferred daily to fresh food and the number of eggs and emerging progeny counted. Of 645 eggs, 628 adult flies emerged, 287 $\gamma$ $B$ females and 341 $\gamma$ $w$ males.

Post-meiotic chromosome loss, however, does account for the disparate sex ratio. This follows from three observations: (1) sperm heads of two different volumes are found in $XY/O$ males; the smaller heads are more frequent than larger heads by the same amount that males are more frequent than females in the progeny. (2) Micronuclei are observed to be formed in, and subsequently eliminated from, spermatids; their size is consonant with the supposition that they contain an $XY$ chromosome, and their frequency exactly accounts for the observed excess of small over large heads. (3) Addition of a $\gamma^+Y$ chromosome to the $XY/O$ constitution eliminates (a) micronucleus formation, (b) the inequality in numbers of large and small heads, and (c) the abnormal sex ratio.

In principle, four phenomena are envisioned that can lead to unequal recovery of reciprocal meiotic products from males: chromosome loss, preferential sperm failure, preferential sperm utilization, and zygotic mortality. (1) Loss of a chromosome leads to generation of a nullosomic gamete. Nullo-sex-chromosome gametes may cause a shift in the sex ratio, whereas a nullo-autosome gamete ordinarily leads to an inviable zygote. Loss of chromosomes may be imagined to arise in several ways; however, only inclusion in micronuclei which are subsequently eliminated is now known to occur in Drosophila. Regardless of

its manner of origin, chromosome loss can never result in the recovery of a homolog in more than half the zygotes (LINDSLEY and SANDLER 1958). (2) Preferential sperm failure, however, frequently results in the recovery of a homolog in more than half the zygotes (LINDSLEY and SANDLER 1958). Sperm failure (i.e., gamete dysfunction, LINDSLEY and SANDLER 1958) may occur at any point between the end of meiosis and fertilization of the egg. These points fall into four classes in the reproductive cycle: sperm development, transmission by the male, storage in the female, and fertilization: (a) Failure of sperm to complete spermiogenesis, i.e., sperm abortion, has been demonstrated in two cases of meiotic drive Segregation Distorter and $In(1)sc^{4L}sc^{8R}/Y$. The consequence of such failure is a decreased appearance of the aborted sperm, hence the genotype they carry, in the sperm pool. (b) Movement of sperm out of testes, into the seminal vesicles, and thus into the female at insemination may be non-random among genotypes. Although conceivable, this phenomenon has not been demonstrated. (c) Sperm deposited in the female may move into the storage organs or remain in the uterus to be eventually swept out at ovoposition. No evidence for non-randomness at this step is known. (d) Sperm that survive the above steps may not be equally efficient in fertilization. (3) Preferential sperm utilization, i.e., non-random utilization of sperm stored in the seminal receptacles, results in a continual change in the composition of the pool. In other words, the probability of recovery of a particular meiotic product will depend on the time from insemination to fertilization, and no sample drawn from the pool will accurately reflect its total composition. (4) Zygotic mortality is ordinarily a function of the genotype of the zygote and unrelated to spermatogenesis except as noted under autosomal loss. Mortality due to sperm dysfunction, although conceivable, has not been demonstrated.

LITERATURE CITED

BAIRATI, A., 1967  Struttura ed ultrastruttura dell' apparato genitae maschile de *Drosophila melanogaster*. Meig. I. Il testicolo. Z. Zellforsch. **76:** 56–99.

BEATTY, R. A. and P. S. BURGOYNE, 1971  Size classes of the head and flagellum of *Drosophila* spermatozoa. Cytogenetics **10:** 177–189.

BEATTY, R. A. and N. S. SIDHU, 1967  Spermatozoan nucleus length in three strains of *Drosophila melanogaster*. Heredity **22:** 65–82. ——, 1970  Polymeagaly of spermatozoan length and its genetic control in *Drosophila* species. Proc. Roy. Soc. Edinburgh B **71:** 14–28.

COHEN, G. and H. EISENBERG, 1968  Deoxyribonucleate solutions: sedimentation in a density gradient, partial specific volumes, density and refractive index increments, and preferential interactions. Biopolymers **6:** 1077–1100.

COOPER, K. W., 1950 Normal spermatogenesis in *Drosophila*. pp. 1–61. In: *Biology of Drosophila*. Edited by M. Demerec. John Wiley, New York.

DAVIS, B. K., 1971 Genetic analysis of a meiotic mutant resulting in precocious sister-centromere separation in *Drosophila melanogaster*. Molec. Gen. Genet. **113**: 251–272.

FAWCETT, D. W., W. A. ANDERSON and D. M. PHILLIPS, 1971 Morphogenetic factors influencing the shape of the sperm head. Devel. Biol. **26**: 220–251.

GERSHENSON, S., 1933 Studies on the genetically inert region of the X-chromosome of Drosophila. I. Behavior of an X-chromosome deficient for a part of its inert region. J. Genet. **28**: 297–313.

HARTL, D. L., Y. HIRAIZUMI and J. F. CROW, 1967 Evidence for sperm dysfunction as the mechanism of Segregation Distortion in *Drosophila melanogaster*. Proc. Natl. Acad. Sci. U.S. **58**: 2240–2245.

HERSKOWITZ, I. H. and H. J. MULLER, 1954 Evidence against a straight end-to-end alignment of chromosomes in Drosophila spermatozoa. Genetics **39**: 836–850.

LINDSLEY, D. L. and E. H. GRELL, 1968 Genetic variations of *Drosophila melanogaster*. Carnegie Inst. Wash. Publ. No. **627**, Washington, D.C.

LINDSLEY, D. L. and L. SANDLER, 1958 The meiotic behavior of grossly deleted X chromosomes in *Drosophila melanogaster*. Genetics **43**: 547–563.

LINDSLEY, D. L., C. W. EDINGTON and E. S. VON HALLE, 1960 Sex-linked recessive lethals in Drosophila whose expression is suppressed by the Y chromosome. Genetics **45**: 1649–1670.

MACGREGOR, H. C. and M. H. WALKER, 1973 The arrangement of chromosomes in nuclei of sperm from plethodontid salamanders. Chromosoma **40**: 243–262.

MCINTOSH, J. R. and K. R. PORTER, 1967 Microtubules in the spermatids of the domestic fowl. J. Cell Biol. **35**: 153–173.

NICOLETTI, B., 1968 Il controllo genetico della meiosi. Atti Assoc. Genet. Ital. **13**: 1–71.

NICOLETTI, B., G. TRIPPA and A. DEMARCO, 1967 Reduced fertility in SD males and its bearing on Segregation Distortion in *Drosophila melanogaster*. Atti Acad. Naz. Lincei **43**: 383–392.

NOVITSKI, E. and I. SANDLER, 1957 Are all products of spermatogenesis regularly functional? Proc. Natl. Acad. Sci. U.S. **43**: 318–324.

OLIVIERI, G. and C. TANZARELLA, 1973 The influence of the nucleolar organizer region on sperm utilization in *Drosophila melanogaster*. Molec. Gen. Genet. **124**: 51–56.

PEACHEY, L. D., 1958 Thin sections I. A study of section thickness and physical distortion produced during microtomy. J. Biophys. Biochem. Cytol. **4**: 233–243.

PEACOCK, W. J., 1965 Nonrandom segregation of chromosomes in *Drosophila* males. Genetics **51**: 573–583.

PEACOCK, W. J. and G. L. G. MIKLOS, 1973 Meiotic drive in Drosophila: new interpretations of the Segregation Distorter and sex chromosome systems. Advan. Genet. **17**: 361–409.

PEACOCK, W. J., K. T. TOKUYASU and R. W. HARDY, 1972 Spermiogenesis and meiotic drive in *Drosophila*. In: *Proc. Int. Symp. The Genetics of the Spermatozoon*. Edited by R. A. BEATTY and S. GLUECKSOHN-WAELSCH. Edinburgh and New York.

PEACOCK, W. J., G. L. G. MIKLOS and D. J. GOODCHILD, 1974 Sex chromosome meiotic drive systems in Drosophila I. Sperm dysfunction in males carrying a heterochromatin-deficient X chromosome. (Submitted for publication.)

PEROTTI, M. E., 1969 Ultrastructure of the mature sperm of *Drosophila melanogaster* Meig. J. Submicro. Cytol. **1**: 171–196.

RASCH, E. M., H. J. BARR and R. W. RASCH, 1971 The DNA content of sperm of *Drosophila melanogaster*. Chromosoma **33**: 1–18.

REYNOLDS, E. S., 1963 The use of lead citrate at high pH as an electron-opaque stain in electron microscopy. J. Cell Biol. **17**: 208–228.

RUDKIN, G. T., 1965 Photometric measurements of individual metaphase chromosomes. In Vitro **1**: 12–20.

SANDLER, L. and G. BRAVER, 1954 The meiotic loss of unpaired chromosomes in *Drosophila melanogaster*. Genetics **39**: 365–377.

SHOUP, J. R., 1967 Spermiogenesis with special reference to nuclear differentiation in wild type and in a male sterility mutant of *Drosophila melanogaster*. J. Cell Biol. **32**: 663–676.

SIDHU, N. S., 1964 A quantitative study of spermatozoon nucleus length in *Drosophila melanogaster* (Meig). Proc. Roy. Soc. Edinburgh B **68**: 327–335.

STANLEY, H. P., J. T. BOWMAN, L. J. ROMWELL, S. C. REED and R. F. WILKINSON, 1972 Fine structure of normal spermatid differentiation in *Drosophila melanogaster*. J. Ultrastruct. Res. **41**: 433–466.

TATES, A. D., 1971 Cytodifferentiation during spermatogenesis in *Drosophila melanogaster*: an electron microscope study. Thesis 'S-Gravenhage: Drukkerij J. H. Pasmans.

TOKUYASU, K. T., 1974 Dynamics of spermiogenesis in *Drosophila melanogaster* IV. Nuclear transformation. J. Ultrastruct. Res. **48**: 284–303.

TOKUYASU, K. T., W. J. PEACOCK and R. W. HARDY, 1972a Dynamics of spermiogenesis in *Drosophila melanogaster* I. Individualization process. Z. Zellforsch. **124**: 479–506. ———, 1972b Dynamics of spermiogenesis in *Drosophila melanogaster* II. Coiling process. Z. Zellforsch. **127**: 492–525.

XUONG, NGUYEN-HUU, 1969 An automatic scanning densitometer and its application to X-ray crystallography. J. Sci. Instrum. (J. Phys. E) **2** (Ser 2): 485–489.

Corresponding editor: G. LEFEVRE